and VF.[1–5,7] In this patient, however, additional medical histories not limited to arrhythmias, such as severe mental retardation, abnormal proliferation of the oesophageal blood vessels, epilepsy, and Kawasaki' disease, were also documented. Because *KCNJ2* is known to be expressed in a variety of tissues, such as cardiac and skeletal muscle, the brain, arterial smooth muscle cells and developing bony structures of the craniofacial region, extremities, and vertebrae,[29–31] some of her compound disorders may be attributed to the *KCNJ2* mutation. In fact, loss-of-function mutations in *KCNJ2* cause Andersen–Tawil syndrome, which is characterized by prolonged repolarization, dysmorphic features, and periodic paralysis.[10,32] In the family of our female patient, we could not perform extensive genetic testing. We cannot exclude the possibility of the presence of other affected genes. Further analyses using knock-in mice or induced pluripotent stem cells would culminate monumental insight into the relationship between the *KCNJ2* M301K mutation and the patient's extra-cardiac phenotypes.

4.6 Conclusions

We described a novel *KCNJ2* gain-of-function mutation, M301K, in a patient with SQTS. Functional assays revealed no functional currents in the homozygous channels, whereas impaired inward rectification in the heterozygous channels manifested in larger outward currents, which is a novel mechanism predisposing SQTS.

Acknowledgements

We thank Dr Richard H. Kaszynski at the Kobe University School of Medicine for his critical reading of this manuscript.

Conflict of interest: none declared.

Funding

This work was supported by research grants from the Ministry of Education, Culture, Science, and Technology of Japan (T.M. and M.H.), the Takeda Science Foundation (T.M.), the Miyata Cardiac Research Promotion Foundation (T.M.), Japan Heart Foundation/Novartis Grant for Research Award on Molecular and Cellular Cardiology (T.M.), the Uehara Memorial Foundation (M.H.), Suzuken Memorial Foundation (T.K.), and health science research grants from the Ministry of Health, Labor, and Welfare of Japan for Clinical Research on Measures for Intractable Diseases (T.M. and M.H.).

References

1. Gussak I, Brugada P, Brugada J, Wright RS, Kopecky SL, Chaitman BR *et al.* Idiopathic short QT interval: a new clinical syndrome? *Cardiology* 2000;**94**:99–102.
2. Brugada R, Hong K, Dumaine R, Cordeiro J, Gaita F, Borggrefe M *et al.* Sudden death associated with short-QT syndrome linked to mutations in HERG. *Circulation* 2004; **109**:30–35.
3. Bellocq C, van Ginneken AC, Bezzina CR, Alders M, Escande D, Mannens MM *et al.* Mutation in the KCNQ1 gene leading to the short QT-interval syndrome. *Circulation* 2004;**109**:2394–2397.
4. Priori SG, Pandit SV, Rivolta I, Berenfeld O, Ronchetti E, Dhamoon A *et al.* A novel form of short QT syndrome (SQT3) is caused by a mutation in the KCNJ2 gene. *Circ Res* 2005;**96**:800–807.
5. Antzelevitch C, Pollevick GD, Cordeiro JM, Casis O, Sanguinetti MC, Aizawa Y *et al.* Loss-of-function mutations in the cardiac calcium channel underlie a new clinical entity characterized by ST-segment elevation, short QT intervals, and sudden cardiac death. *Circulation* 2007;**115**:442–449.
6. Templin C, Ghadri JR, Rougier JS, Baumer A, Kaplan V, Albesa M *et al.* Identification of a novel loss-of-function calcium channel gene mutation in short QT syndrome (SQTS6). *Eur Heart J* 2011;**32**:1077–1088.
7. Hong K, Piper DR, Diaz-Valdecantos A, Brugada J, Oliva A, Burashnikov E *et al.* De novo KCNQ1 mutation responsible for atrial fibrillation and short QT syndrome in utero. *Cardiovasc Res* 2005;**68**:433–440.
8. Garberoglio L, Giustetto C, Wolpert C, Gaita F. Is acquired short QT due to digitalis intoxication responsible for malignant ventricular arrhythmias? *J Electrocardiol* 2007; **40**:43–46.
9. Akao M, Ohler A, O'Rourke B, Marban E. Mitochondrial ATP-sensitive potassium channels inhibit apoptosis induced by oxidative stress in cardiac cells. *Circ Res* 2001; **88**:1267–1275.
10. Haruna Y, Kobori A, Makiyama T, Yoshida H, Akao M, Doi T *et al.* Genotype-phenotype correlations of KCNJ2 mutations in Japanese patients with Andersen-Tawil syndrome. *Hum Mutat* 2007;**28**:208.
11. Ma D, Tang XD, Rogers TB, Welling PA. An Andersen-Tawil syndrome mutation in Kir2.1 (V302M) alters the G-loop cytoplasmic K+ conduction pathway. *J Biol Chem* 2007;**282**:5781–5789.
12. Ballester LY, Benson DW, Wong B, Law IH, Mathews KD, Vanoye CG *et al.* Trafficking-competent and trafficking-defective KCNJ2 mutations in Andersen syndrome. *Hum Mutat* 2006;**27**:388.
13. Pegan S, Arrabit C, Zhou W, Kwiatkowski W, Collins A, Slesinger PA *et al.* Cytoplasmic domain structures of Kir2.1 and Kir3.1 show sites for modulating gating and rectification. *Nat Neurosci* 2005;**8**:279–287.
14. Tai K, Stansfeld PJ, Sansom MS. Ion-blocking sites of the Kir2.1 channel revealed by multiscale modeling. *Biochemistry* 2009;**48**:8758–8763.
15. Fujiwara Y, Kubo Y. Functional roles of charged amino acid residues on the wall of the cytoplasmic pore of Kir2.1. *J Gen Physiol* 2006;**127**:401–419.
16. Gollob MH, Redpath CJ, Roberts JD. The short QT syndrome: proposed diagnostic criteria. *J Am Coll Cardiol* 2011;**57**:802–812.
17. Xia M, Jin Q, Bendahhou S, He Y, Larroque MM, Chen Y *et al.* A Kir2.1 gain-of-function mutation underlies familial atrial fibrillation. *Biochem Biophys Res Commun* 2005;**332**:1012–1019.
18. Matsuda H, Saigusa A, Irisawa H. Ohmic conductance through the inwardly rectifying K channel and blocking by internal Mg2+. *Nature* 1987;**325**:156–159.
19. Horie M, Irisawa H, Noma A. Voltage-dependent magnesium block of adenosine-triphosphate-sensitive potassium channel in guinea-pig ventricular cells. *J Physiol* 1987;**387**:251–272.
20. Hille B. *Ion Channels of Excitable Membranes*. Sunderland: Sinauer Associates, 2001.
21. Robertson JL, Palmer LG, Roux B. Long-pore electrostatics in inward-rectifier potassium channels. *J Gen Physiol* 2008;**132**:613–632.
22. Liu Y, Fowler CD, Wang Z. Ontogeny of brain-derived neurotrophic factor gene expression in the forebrain of prairie and montane voles. *Brain Res Dev Brain Res* 2001; **127**:51–61.
23. Nakamura TY, Artman M, Rudy B, Coetzee WA. Inhibition of rat ventricular IK1 with antisense oligonucleotides targeted to Kir2.1 mRNA. *Am J Physiol* 1998;**274**: H892–H900.
24. Picones A, Keung E, Timpe LC. Unitary conductance variation in Kir2.1 and in cardiac inward rectifier potassium channels. *Biophys J* 2001;**81**:2035–2049.
25. Wible BA, De Biasi M, Majumder K, Taglialatela M, Brown AM. Cloning and functional expression of an inwardly rectifying K+ channel from human atrium. *Circ Res* 1995;**76**: 343–350.
26. Preisig-Muller R, Schlichthorl G, Goerge T, Heinen S, Bruggemann A, Rajan S *et al.* Heteromerization of Kir2.x potassium channels contributes to the phenotype of Andersen's syndrome. *Proc Natl Acad Sci USA* 2002;**99**:7774–7779.
27. Miake J, Marban E, Nuss HB. Functional role of inward rectifier current in heart probed by Kir2.1 overexpression and dominant-negative suppression. *J Clin Invest* 2003;**111**:1529–1536.
28. Viswanathan MN, Page RL. Short QT: when does it matter? *Circulation* 2007;**116**: 686–688.
29. Raab-Graham KF, Radeke CM, Vandenberg CA. Molecular cloning and expression of a human heart inward rectifier potassium channel. *Neuroreport* 1994;**5**:2501–2505.
30. Karkanis T, Li S, Pickering JG, Sims SM. Plasticity of KIR channels in human smooth muscle cells from internal thoracic artery. *Am J Physiol Heart Circ Physiol* 2003;**284**: H2325–H2334.
31. Karschin C, Karschin A. Ontogeny of gene expression of Kir channel subunits in the rat. *Mol Cell Neurosci* 1997;**10**:131–148.
32. Plaster NM, Tawil R, Tristani-Firouzi M, Canun S, Bendahhou S, Tsunoda A *et al.* Mutations in Kir2.1 cause the developmental and episodic electrical phenotypes of Andersen's syndrome. *Cell* 2001;**105**:511–519.

Successful Catheter Ablation of Bidirectional Ventricular Premature Contractions Triggering Ventricular Fibrillation in Catecholaminergic Polymorphic Ventricular Tachycardia With *RyR2* Mutation

Takashi Kaneshiro, MD; Yoshihisa Naruse, MD; Akihiko Nogami, MD; Hiroshi Tada, MD; Kentaro Yoshida, MD; Yukio Sekiguchi, MD; Nobuyuki Murakoshi, MD; Yoshiaki Kato, MD; Hitoshi Horigome, MD; Mihoko Kawamura, MD; Minoru Horie, MD; Kazutaka Aonuma, MD

The subject of this report is a 38-year-old woman who often experienced syncope since childhood. Syncope occurred >10 times a year and was associated with convulsion during exercise and emotionally exciting situations. The patient's 13-year-old daughter had also experienced frequent episodes of syncope and developed ventricular fibrillation (VF) during treadmill exercise testing that was successfully defibrillated with electric shock. Witnessing this situation, the patient also lost consciousness, with documented VF that was converted to sinus rhythm by cardiopulmonary resuscitation without electric defibrillation.

Both the patient and her daughter were admitted to our hospital. We performed echocardiography, coronary angiography, and cardiac CT, the results of which revealed no structural heart disease. Resting 12-lead ECG did not indicate any abnormalities, including long-QT syndrome or Brugada syndrome. A signal-averaged ECG revealed no late potentials. Treadmill exercise testing easily induced bigeminal ventricular premature contractions (VPCs) with a right bundle branch block configuration and inferior axis (Figure 1A), and the exercise was terminated because of intolerable symptoms. Catecholamine stress test was started with administration of continuous intravenous infusion of epinephrine in a stepwise manner from 0.025 μg/kg per minute.[1] During epinephrine infusion at a rate of 0.1 μg/kg per minute, multifocal VPCs (VPC #1, right bundle branch block configuration and superior axis; VPC #2, right bundle branch block configuration and inferior axis [the same VPC configuration as that induced during the treadmill exercise testing]; and VPC #3, left bundle branch block configuration and inferior axis) appeared, and VPC #1 following VPC #2 subsequently induced VF (Figure 1B).

Administration of bisoprolol 5 mg QD was given but failed to suppress the exercise-induced bigeminal VPCs with the same morphology as induced previously. Because frequent deliveries of shock were believed to be likely, even with β-blocker treatment, catheter ablation was offered to the patient before implantable cardioverter-defibrillator (ICD) implantation. Catheter mapping and ablation for the bidirectional VPCs were performed with a 3D electroanatomic mapping system (CARTO; Biosense Webster) and a 3.5-mm-tip irrigation catheter (NaviStar; Thermo Cool) with only local anesthesia. No VPCs, ventricular tachycardia (VT), or VF were inducible with burst pacing and programmed stimulation from both right ventricular apex and right outflow tract during baseline and continuous intravenous infusion of isoproterenol.

With epinephrine infusion at a rate of 0.1 μg/kg per minute, VPC #1 and VPC #2 appeared. VPC #1 was nonsustained, and a presystolic Purkinje potential was recorded at the left ventricular inferoseptal area near the posteromedial papillary muscle, which preceded the onset of VPC #1 by 18 ms. The unipolar electrogram from the ablation catheter during VPC #1 showed a QS pattern, and a perfect match of the QRS configuration was obtained by pace mapping (Figure 2). Radiofrequency energy application to this site provoked some ventricular acceleration beats, and several radiofrequency energy applications around the target site finally eliminated all the VPCs, resulting in complete suppression of all VPC #1.

After the ablation of VPC #1, isolated occurrences of VPC #2 continued, and a local bipolar electrogram recorded on the left coronary cusp showed discrete prepotential that preceded the onset of VPC #2 by 65 ms, and a perfect match of the

Received July 26, 2011; accepted January 5, 2012.

From the Cardiovascular Division, Institute of Clinical Medicine (T.K., Y.N., H.T., K.Y., Y.S., N.M., K.A.) and Department of Child Health (Y.K., H.H.), Graduate School of Comprehensive Human Sciences, University of Tsukuba, Tsukuba, Japan; Division of Heart Rhythm Management, Yokohama Rosai Hospital, Yokohama, Japan (A.N.); and Department of Cardiovascular and Respiratory Medicine, Shiga University of Medical Science, Shiga, Japan (M.K., M.H.).

Correspondence to Kazutaka Aonuma, MD, Cardiovascular Division, Institute of Clinical Medicine, Graduate School of Comprehensive Human Sciences, University of Tsukuba, 1-1-1 Tennodai, Tsukuba, Ibaraki 305-8575, Japan. E-mail kaonuma@md.tsukuba.ac.jp

(*Circ Arrhythm Electrophysiol.* **2012;5:e14-e17.**)

Circ Arrhythm Electrophysiol **is available at http://circep.ahajournals.org** **DOI: 10.1161/CIRCEP.111.966549**

Figure 1. A, Twelve-lead ECG recording during treadmill exercise testing. Bigeminal ventricular premature contractions (VPCs) appeared during the second stage of the Bruce protocol. VPC morphology represented a right bundle branch block configuration and inferior axis. Because the patient experienced intolerable symptoms, the test was discontinued. **B**, Epinephrine stress test. Continuous intravenous infusion of epinephrine was started from a rate of 0.025 μg/kg per minute, and the QT interval did not changed. At a rate of 0.1 μg/kg per minute, VPC #1 (right bundle branch block configuration and superior axis), VPC #2 (right bundle branch block configuration and inferior axis, same as that induced in the treadmill exercise testing), and VPC #3 (left bundle branch block configuration and inferior axis) were induced. Subsequently, VPC #1 following VPC #2 suddenly induced ventricular fibrillation, which was successfully terminated with electric shock.

QRS configuration was obtained by pace mapping (Figure 3). Radiofrequency energy application to the left coronary cusp abolished VPC #2 4 s after the onset of radiofrequency energy application. After successful catheter ablation of bidirectional VPCs, neither VPCs nor VF were inducible, even with an infusion of epinephrine of up to 1.2 μg/kg per minute (a >10 times higher dose than provocation). Precise ablation sites in a 3D electroanatomic mapping merged with contrast-enhanced CT are shown in Figure 4.

ICD implantation was performed, and the patient was discharged from the hospital on bisoprolol 2.5 mg QD. Serial Holter ECGs after the ablation showed only 3 to 5 isolated VPCs with a different morphology from the previously observed VPCs, and treadmill exercise testing induced no VPCs at the maximal workload. During 16-month follow-up, neither episodes of syncope nor ICD therapy occurred. Genetic analysis revealed a mutation in the ryanodine receptor gene (*RyR2*), and a diagnosis of catecholaminergic polymorphic VT (CPVT) was confirmed (Figure 5).[2] The patient's daughter was also given a diagnosis of CPVT with same mutation in *RyR2* and had catheter ablation for the origins of bidirectional VT. Although she refused ICD

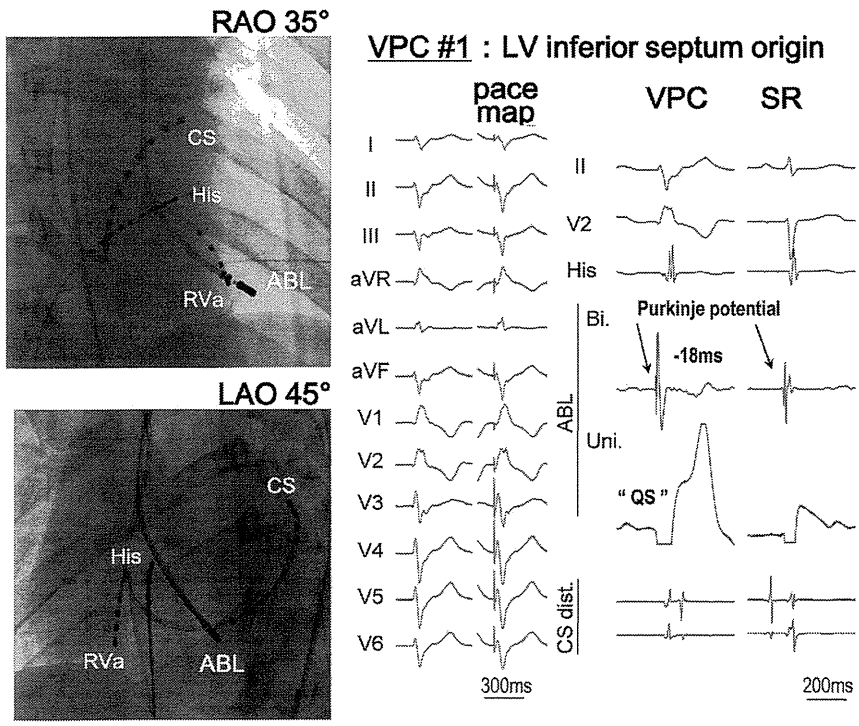

Figure 2. Activation mapping and pace mapping for VPC #1. A Purkinje potential was recorded from the left ventricular inferoseptum and preceded the QRS onset by 18 ms. The unipolar electrogram recorded from the distal electrode showed a QS pattern. Perfect pace mapping was obtained at this site. ABL indicates ablation catheter; CS, coronary sinus; His, His bundle; LAO, left anterior oblique; RAO, right anterior oblique; RVa, right ventricular apex; SR, sinus rhythm; VPC, ventricular premature contraction.

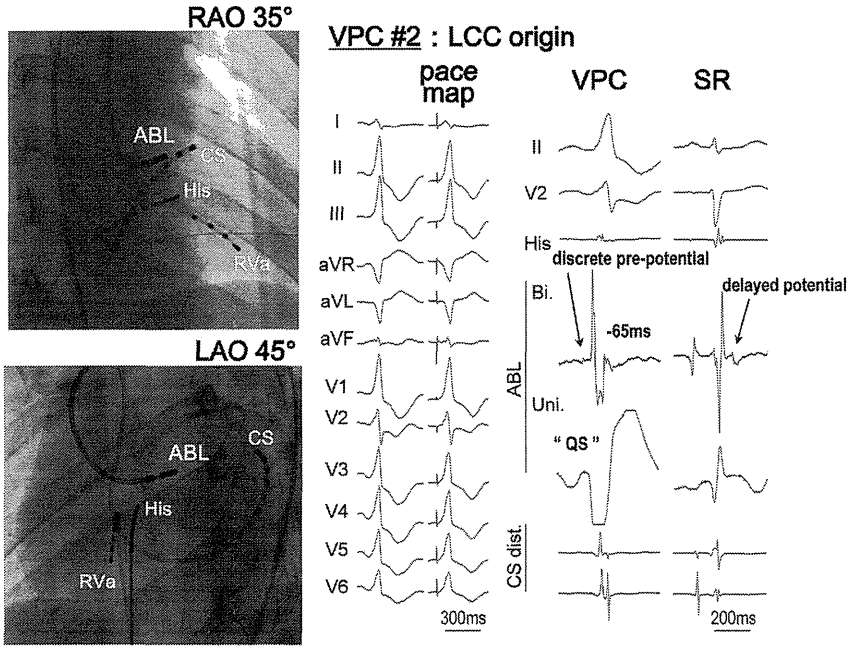

Figure 3. Activation mapping and pace mapping for VPC #2. A local bipolar electrogram recorded from the LCC showed a discrete prepotential that preceded the QRS onset by 65 ms associated with a QS pattern of unipolar electrogram. Perfect pace mapping was obtained at this site. ABL indicates ablation catheter; CS, coronary sinus; His, His bundle; LAO, left anterior oblique; LCC, left coronary cusp; RAO, right anterior oblique; RVa, right ventricular apex; SR, sinus rhythm; VPC, ventricular premature contraction.

implantation, she had not experienced any episode of VT or syncope with β-blocker treatment.

The generally accepted therapy for CPVT has been β-blockers,[3] and the additional administration of flecainide or verapamil to β-blockers has been reported to be effective; however, the effects of those drugs are not fully standardized. For medically refractory cases, sympathetic denervation is one of the alternative treatment options. The ICD is considered the definitive therapy for the prevention of sudden cardiac death; however, failure to prevent sudden cardiac death has been reported in several cases because ICD shock delivery might lead to catecholamine release, resulting in an electric storm.[4] This concern prompted the decision to attempt catheter ablation of VPCs triggering VF. Although several reports have described successful catheter ablation of VPCs triggering VF in some patients with structurally normal hearts, such as those with Brugada syndrome, long-QT syndrome, and idiopathic VF, successful catheter ablation of VPCs triggering VF in CPVT has not been reported. Cerrone and colleagues[5] reported that the mechanism of CPVT was due to the delayed afterdepolarization-induced triggered activity in a focal Purkinje network in a knock-in (*RyR2*) mouse. However, whether the Purkinje system is related to the mechanism of VF in CPVT or just trigger origin is still unknown.

To our knowledge, this is the first report of successful catheter ablation of the bidirectional VPCs that trigger VF, and this procedure could become one of the adjunctive

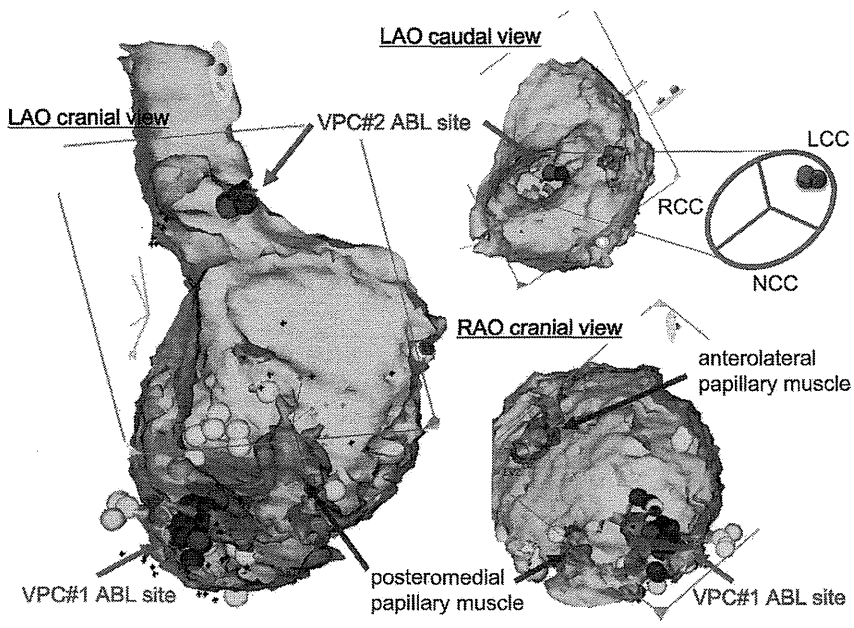

Figure 4. Electroanatomic mapping merged with contrast-enhanced CT. Red tags indicate the ABL sites. Blue tags indicate the sites with perfect pace mapping, and yellow tags indicate the sites with Purkinje potentials during sinus rhythm. The sites with perfect pace mapping and the earliest activation for VPC #1 were localized in the inferoseptal site adjacent to the base of the posteromedial papillary muscle (red arrow). Successful ablation site of VPC #2 was on the left coronary cusp (blue arrow). ABL indicates ablation; LAO, left anterior oblique; LCC, left coronary cusp; NCC, noncoronary cusp; RAO, right anterior oblique; RCC, right coronary cusp; VPC, ventricular premature contraction.

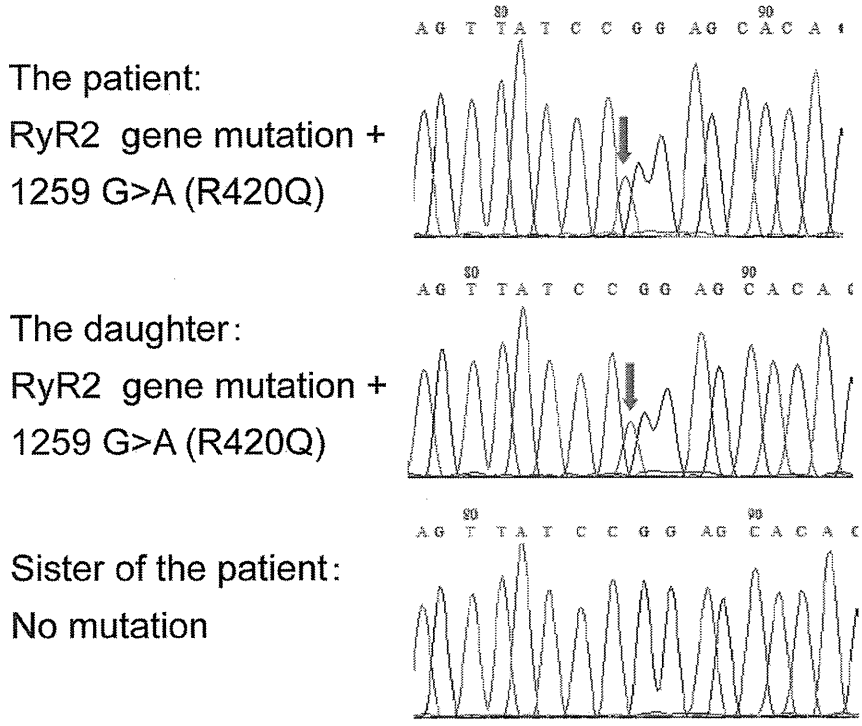

Figure 5. Results of genetic analysis. A mutation in the ryanodine receptor gene (*RyR2*) was detected in both the patient and her daughter. The mutation was not detected in the patient's sister.

therapies in patients with CPVT. To clarify the effectiveness and safety of this procedure, more cases and longer-term observation are mandatory.

Disclosures

None.

References

1. Krahn AD, Gollob M, Yee R, Gula LJ, Skanes AC, Walker BD, Klein GJ. Diagnosis of unexplained cardiac arrest: role of adrenaline and procainamide infusion. *Circulation.* 2005;112:2228–2234.
2. Priori SG, Napolitano C, Tiso N, Memmi M, Vignati G, Bloise R, Sorrentino V, Danieli GA. Mutations in the cardiac ryanodine receptor gene (*hRyR2*) underlie catecholaminergic polymorphic ventricular tachycardia. *Circulation.* 2001;103:196–200.
3. Sumitomo N, Harada K, Nagashima M, Yasuda T, Nakamura Y, Aragaki Y, Saito A, Kurosaki K, Jouo K, Koujiro M, Konishi S, Matsuoka S, Oono T, Hayakawa S, Miura M, Ushinohama H, Shibata T, Niimura I. Catecholaminergic polymorphic ventricular tachycardia: electrocardiographic characteristics and optimal therapeutic strategies to prevent sudden death. *Heart.* 2003;89:66–70.
4. Mohamed U, Gollob MH, Gow RM, Krahn AD. Sudden cardiac death despite an implantable cardioverter-defibrillator in a young female with catecholaminergic ventricular tachycardia. *Heart Rhythm.* 2006;3:1486–1489.
5. Cerrone M, Noujaim SF, Tolkacheva EG, Talkachou A, O'Connell R, Berenfeld O, Anumonwo J, Pandit SV, Vikstrom K, Napolitano C, Priori SG, Jalife J. Arrhythmogenic mechanisms in a mouse model of catecholaminergic polymorphic ventricular tachycardia. *Circ Res.* 2007;101:1039–1048.

KEY WORDS: catecholaminergic polymorphic ventricular tachycardia ■ catheter ablation ■ arrhythmia

Circulation Journal
Official Journal of the Japanese Circulation Society
http://www.j-circ.or.jp

ORIGINAL ARTICLE
Arrhythmia/Electrophysiology

Prognostic Implications of Progressive Cardiac Conduction Disease

Tamiro Kawaguchi, MD; Hideki Hayashi, MD, PhD; Akashi Miyamoto, MD, PhD; Tomohide Yoshino, MD; Atsushi Taniguchi, MD; Nobu Naiki, MD; Yoshihisa Sugimoto, MD, PhD; Makoto Ito, MD, PhD; Joel Q. Xue, PhD; Yoshitaka Murakami, PhD; Minoru Horie, MD, PhD

Background: Progressive cardiac conduction disease (PCCD), characterized by temporal increase in PR interval and QRS duration, may be attributed to diverse pathophysiological mechanisms. This study aimed to investigate whether PCCD is associated with increased risk of cardiovascular morbidity and mortality.

Methods and Results: Digital analysis of 12-lead ECG was performed to select patients with PCCD from among a database containing 359,737 ECGs. Long-term prognosis of PCCD was assessed in a large hospital-based population: 458 patients (341 males; mean age, 57.9±14.7 years) with PCCD were enrolled. During a mean follow-up of 13.3±6.4 years, 109 patients were hospitalized for heart failure (HF), and there were 16 and 59 deaths from cardiovascular diseases and all causes, respectively. Multivariate Cox proportional hazards analysis confirmed (1) a significant association of temporal incremental rate of PR interval (≥2 ms/year) and QRS duration (≥3 ms/year) with HF hospitalization (hazard ratio [HR], 2.34; 95% confidence interval [CI], 1.36–4.05; P=0.002 and HR, 2.08; 95% CI, 1.25–3.53; P=0.01, respectively) and (2) a significant association of temporal incremental rate of PR interval (≥4 ms/year) and QRS duration (≥5 ms/year) with cardiovascular mortality (HR, 6.9; 95% CI, 1.47–36.96; P=0.02 and HR, 4.31; 95% CI, 1.19–16.5; P=0.03, respectively).

Conclusions: The severity of PCCD was independently and significantly associated with HF hospitalization and cardiovascular mortality. (*Circ J* 2013; **77:** 60–67)

Key Words: Conduction; Electrocardiography; Heart failure; Prognosis; Ventricles

Progressive cardiac conduction disease (PCCD) is characterized by electrical deterioration of the conduction system in the atrium and ventricle, thus presenting as temporal prolongation of the PR interval and QRS duration. Lev and Unger[1] and Lenègre[2] reported pathological abnormalities in the conduction system with deposition of fibrous tissue in patients who developed ventricular conduction disturbance. On the other hand, inherited arrhythmias, including sick sinus syndrome, atrioventricular block and bundle branch block, have been reported. Several genetic abnormalities have been found in patients with inherited cardiac conduction abnormalities,[3] but although these disorders exhibit remarkable clinical characteristics such as syncope, sudden death and pacemaker implantation requirement, the prevalence is rare.

Editorial p41

In contrast, the relation of QRS duration with an increased rate of mortality[4,5] and reduced left ventricular ejection function[6] has been studied in numerous patients with and without ischemic heart diseases. In patients with myocardial infarction and reduced cardiac function, the benefit from implantable-cardioverter defibrillator therapy is higher when the QRS duration is longer.[7] These findings suggest that PCCD plays an important role in determining the prognosis of various cardiac disorders, including ischemic and nonischemic heart diseases.

However, little is known about the effect of temporal deterioration of supra- and intraventricular conduction on prognosis in a large hospital-based population. In Shiga University of Medical Science's hospital, more than 350,000 ECGs obtained from more than 100,000 patients are available for digital analysis. The long-term outcomes are precisely identified by the medical records. Using this large database, we systematically examined the association of PCCD with cardiovascular morbidity and mortality. This study also benefited from reproducible ECG measures based on computer-processed analyses.

Received July 2, 2012; revised manuscript received August 3, 2012; accepted August 23, 2012; released online September 26, 2012 Time for primary review: 8 days

Department of Cardiovascular and Respiratory Medicine (T.K., H.H., A.M., T.Y., A.T., N.N., Y.S., M.I., M.H.), Department of Medical Statistics (Y.M.), Shiga University of Medical Science, Otsu, Japan; and General Electric Healthcare, Milwaukee, WI (J.Q.X.), USA

Mailing address: Hideki Hayashi, MD, PhD, Department of Cardiovascular and Respiratory Medicine, Shiga University of Medical Science, Otsu 520-2192, Japan. E-mail: hayashih@belle.shiga-med.ac.jp

ISSN-1346-9843 doi:10.1253/circj.CJ-12-0849

Methods

The research protocol was approved by the Ethical Committee of Shiga University of Medical Science.

Study Population

In the University's hospital, digital recording of 12-lead ECGs started in January 1983. Until July 2010, a total of 114,334 consecutive patients (55,091 females and 59,243 males) underwent 12-lead ECG recordings in the supine position. The ECG database comprises a total of 359,737 ECGs collected during that period. The 12-lead ECG was recorded at rest for 10 s at a sweep speed of 25 mm/s, calibrated to 1 mV/cm in the standard leads. The data were digitally stored in a 12-bit server computer with a sampling interval of 2 ms.

From the database, we chose patients who exhibited wide QRS duration ≥120 ms between January 2000 and December 2003, enrolled in this study with the last follow-up on December 2010. To determine the temporal increase in QRS duration, the time interval of serial ECG recordings was at least ≥1 year. ECGs exhibiting Wolff-Parkinson-White syndrome, ventricular pacing, junctional or idioventricular rhythm and ventricular tachyarrhythmias were excluded. Patients who were <15 years old were also excluded from the analysis.

ECG Analysis

The ECG analysis was performed using software (MUSE7.1, GE Marquette Medical Systems, Inc, Milwaukee, WI, USA). Standardized, computerized ECG criteria as described by a 12-lead ECG analysis program were used to diagnose abnormal intraventricular morphologies. ECG variables, including duration, interval, amplitude, and axis, were digitally measured. For the ECG measurement, a median complex was computed as follows: (1) all QRS complexes of the same morphology were aligned in time and (2) the algorithm generated a representative QRS complex from the median voltages that were found at each successive sample time. QRS duration was measured from the earliest detection of depolarization in any lead (QRS onset) to the latest detection of depolarization in any lead (QRS offset). PR interval was measured in a similar manner. Because all variables of the 12-lead ECG were digitally measured based on computer-processed analysis, neither intra- nor interobserver variability needed to be taken into account and all measures were reproducible.

Follow-up

The follow-up period of all patients started from the day of the first ECG recording. We explored the prognostic factors for the endpoints of this study: cardiovascular death, all-cause death, and heart failure (HF) hospitalization. The outcome was assessed by searching the medical records in the hospital database. The determination of HF hospitalization was based on review of the hospital records. HF hospitalization had to satisfy both of the following criteria: (1) admission to hospital for ≥24 h with a clinical history of worsening symptoms of HF as evidenced by clinical criteria, including increased New York Heart Association functional class, orthopnea, paroxysmal nocturnal dyspnea, edema, exertional dyspnea, or gastrointestinal symptoms attributable to HF, and (2) one or more intensive treatments for HF within 24 h of admission, such as intravenous diuretics or inotropic agents. All ECGs taken during the follow-up were evaluated in patients enrolled in this study. The first ECG recording was assigned as the baseline ECG. The ECG recording in which the QRS duration was longest during follow-up was defined as the follow-up ECG.

Table 1. Baseline Demographics of the Patients

Total patients, n	458
Age (years)	57.9±14.7
Sex, male (%)	341 (74.5)
Follow-up period of ECG (years)	9.0±5.7
Survival period (years)	13.3±6.4
HF, n (%)	42 (9.2)
Ischemic heart disease, n (%)	55 (12.0)
Cardiomyopathy, n (%)	14 (3.1)
Hypertension, n (%)	160 (34.9)
Diabetes mellitus, n (%)	96 (21.0)
Valvular heart disease, n (%)	19 (4.1)
AF, n (%)	29 (6.3)
Arrhythmias*, n (%)	30 (6.6)
Malignant disease, n (%)	32 (7.0)
Cardiovascular surgery, n (%)	38 (8.3)
Other†, n (%)	31 (6.8)

Data are presented as mean±standard deviation and n (%).
*Arrhythmia involves patients with various types of rhythm disorder except for patients who exhibited AF when the ECG was recorded.
†Includes patients who suffered various internal diseases.
HF, heart failure; AF, atrial fibrillation.

Statistical Analysis

We described continuous variables using mean and standard deviation, and categorical variables using number and percentage. Comparisons between groups were made by t-test for continuous variables and χ^2 test for categorical variables. A receiver-operating characteristic curve was used to determine the cutoff point of prognostic factors that optimized the sensitivity and specificity of ECG variables for the endpoints. A Kaplan-Meier curve was created to describe the event-free survival rate and differences between groups were compared by log-rank test. Cox proportional hazards models were used to estimate hazard ratios of HF hospitalization, cardiovascular mortality and all-cause mortality adjusted by age, sex, and other confounding factors. Variables included in the Cox model were selected by a variable procedure with a criteria of $P<0.1$ for exclusion. All tests were 2-tailed and the significance level was set at 0.05. Because this study primarily evaluated cardiac conduction, we repeated the statistical analyses with patients without nodal-blocking agents such as β-blockers, Vaughan-Williams classes I, III, and IV anti-arrhythmic drugs, digitalis, and H2 histamine-blocker.

Results

A total of 458 consecutive patients (341 men; mean age, 57.9±14.7 years) were enrolled in this study. Among them, 109 (23.8%) were hospitalized because of HF. In addition, 59 (12.9%) patients died, of which cardiovascular death occurred in 16 (3.5%) patients. The mean duration of follow-up was 13.3±6.4 years.

Clinical Characteristics of the Patients

Table 1 shows the baseline clinical characteristics of the patients enrolled in this study. The study population consisted of patients with various cardiac diseases and other disorders including diabetes, malignancy, and surgery. The number of ECG recordings averaged 17.8±21 (median: 11) per patient. Table 2 shows 12-lead ECG measures and morphological characteris-

Table 2. Characteristics of 12-Lead ECGs

	First ECG	Follow-up ECG	Temporal change*	P value
ECG measures				
Heart rate (beats/min)	68.6±14.1	66.1±13.1	−2.7±15.5	0.01
PR interval (ms)	165.0±27.4	178.5±34.0	13.9±20.2	<0.0001
QRS duration (ms)	118.9±22.8	142.9±15.4	24.0±22.5	<0.0001
QRS morphology				
Normal (n, %)	143, 31.2	0, 0	−31.2	<0.0001
RBBB (n, %)	186, 40.6	297, 64.8	24.2	<0.0001
RBBB with LAH (n, %)	13, 2.8	37, 8.1	5.3	0.0004
LBBB (n, %)	31, 6.8	47, 10.3	3.5	0.06
NSIVCD (n, %)	85, 18.6	76, 16.6	−2.0	0.43

Data are presented as mean±standard deviation and n (%).
*Temporal change indicates the difference in ECG measures or the prevalence of QRS morphology between the baseline ECG and the follow-up ECG.
RBBB, right bundle branch block; LAH, left anterior hemiblock; LBBB, left bundle branch block; NSIVCD, nonspecific intraventricular conduction disturbance.

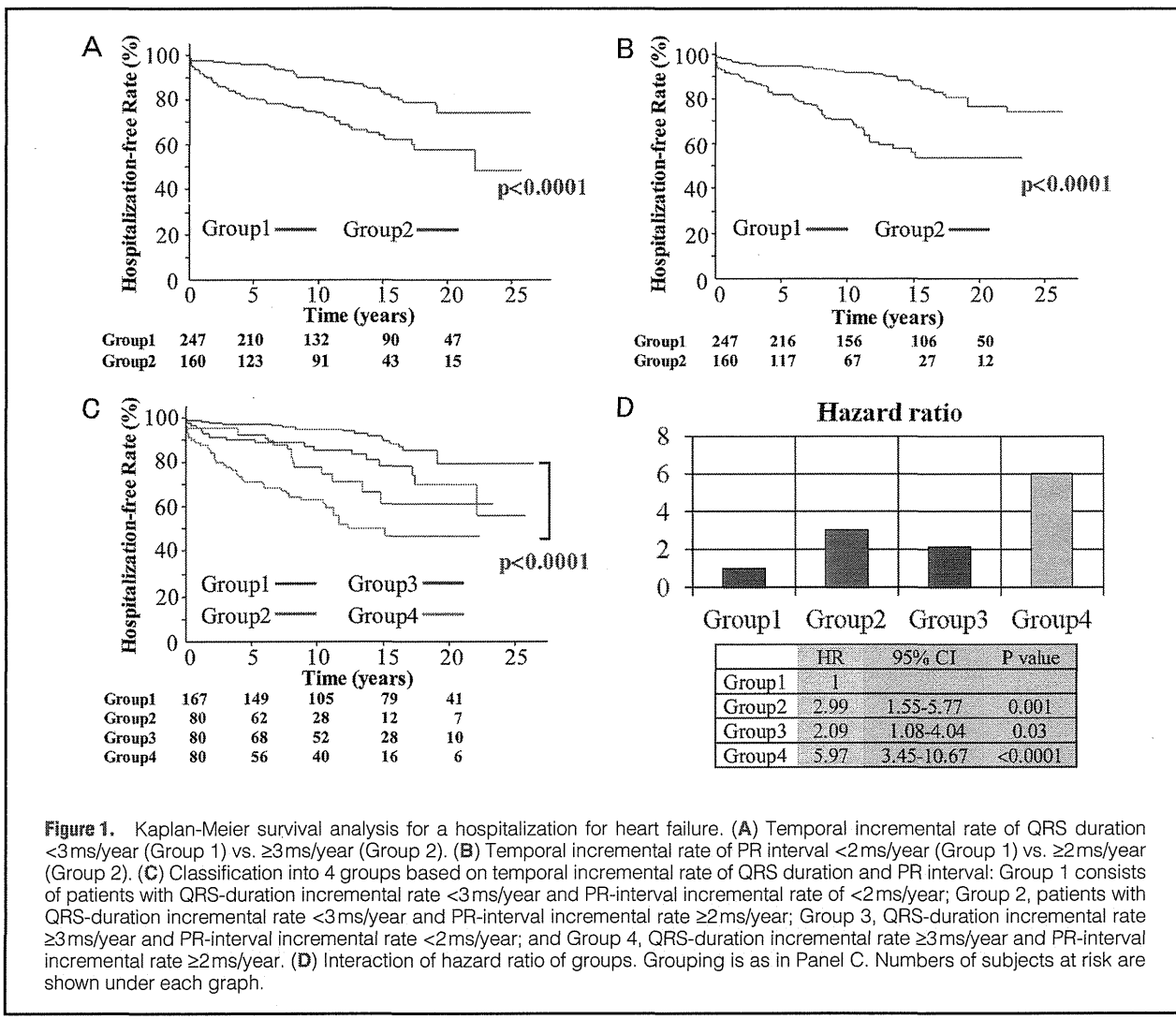

Figure 1. Kaplan-Meier survival analysis for a hospitalization for heart failure. (**A**) Temporal incremental rate of QRS duration <3ms/year (Group 1) vs. ≥3ms/year (Group 2). (**B**) Temporal incremental rate of PR interval <2ms/year (Group 1) vs. ≥2ms/year (Group 2). (**C**) Classification into 4 groups based on temporal incremental rate of QRS duration and PR interval: Group 1 consists of patients with QRS-duration incremental rate <3ms/year and PR-interval incremental rate of <2ms/year; Group 2, patients with QRS-duration incremental rate <3ms/year and PR-interval incremental rate ≥2ms/year; Group 3, QRS-duration incremental rate ≥3ms/year and PR-interval incremental rate <2ms/year; and Group 4, QRS-duration incremental rate ≥3ms/year and PR-interval incremental rate ≥2ms/year. (**D**) Interaction of hazard ratio of groups. Grouping is as in Panel C. Numbers of subjects at risk are shown under each graph.

Table 3. Univariate and Multivariate Survival Analyses of HF Hospitalization

	Univariate analysis (n=407)		Multivariate analysis (n=407)*		Multivariate analysis except nodal-blocking drugs (n=337)†	
	P value	HR (95% CI)	P value	HR (95% CI)	P value	HR (95% CI)
Age (<61 years=1)	0.04	1.55 (1.02–2.36)	0.18	1.37 (0.86–2.20)	0.16	1.47 (0.86–2.55)
Sex (female=1)	0.19	1.38 (0.86–2.33)	0.67	1.12 (0.67–1.95)	0.30	1.37 (0.76–2.57)
Heart rate (<66 beats/min=1)	0.21	1.30 (0.86–1.97)	0.26	1.29 (0.83–2.01)	0.29	1.34 (0.88–2.08)
Incremental rate of QRS duration (<3 ms/year=1)	<0.0001	2.52 (1.66–3.87)	0.01	1.79 (1.15–2.80)	0.01	2.08 (1.25–3.53)
Incremental rate of PR interval (<2 ms/year=1)	<0.0001	3.39 (2.22–5.23)	0.001	2.25 (1.42–3.58)	0.002	2.34 (1.36–4.05)

*Adjusted for age, sex, heart rate, arrhythmia except AF, nodal-blocking drugs, incremental rate of QRS duration, incremental rate of PR interval, diabetes mellitus, ischemic heart disease, and cardiomyopathy.
†Adjusted for age and sex, heart rate, arrhythmia except AF, incremental rate of QRS duration, incremental rate of PR interval, diabetes mellitus, ischemic heart disease, and cardiomyopathy.
HR, hazard ratio; CI, confidence interval. Other abbreviations as in Table 1.

tics of the QRS complex in the baseline and follow-up ECGs. Heart rate was significantly slower in the follow-up ECG than in the baseline ECG. PR interval and QRS duration significantly increased by 8.4% and 20.2%, respectively, during follow-up. In the baseline ECG, normal QRS duration was present in 31.2% of the study population, and right bundle branch block (RBBB), RBBB with left anterior hemiblock (LAH), left bundle branch block (LBBB), or nonspecific intraventricular conduction disturbance (NSIVCD) was present in the remaining patients. During the follow-up, RBBB, RBBB with LAH, and LBBB developed in 99 (21.6%), 9 (2.0%), and 22 (4.8%), respectively, of the patients who showed normal QRS duration in the baseline ECG. The prevalence of RBBB with or without LAH was significantly higher in the follow-up ECG than in the baseline ECG. The prevalence of LBBB showed a trend to increase during the follow-up, but the prevalence of NSIVCD did not significantly alter.

Long-Term Prognosis

HF The most common cause of the endpoints was HF hospitalization. During the follow-up period, 109 patients were hospitalized because of HF. At baseline, age was significantly higher in patients with HF hospitalization than in those without (60.7±11.2 vs. 57.0±15.5 years; P=0.02), but the sex prevalence was not significantly different between the 2 groups (76% vs. 74% male; P=0.64). The prevalence of ischemic heart disease, cardiomyopathy, valvular heart disease, and various arrhythmias excluding atrial fibrillation (AF) was significantly higher in patients with HF hospitalization than in those without (P<0.05 for each). The prevalence of diabetes and AF was marginally higher in patients with HF hospitalization than in those without (P=0.10 and 0.08, respectively). The follow-up period was not significantly different between patients with and without HF hospitalization (13.8±6.2 vs. 13.2±6.5 years, P=0.37). **Table S1** shows the ECG characteristics. In the baseline ECG, heart rate was significantly faster and QRS duration significantly shorter in patients with HF hospitalization than in those without, but the PR interval did not differ between patients with and without HF hospitalization. The prevalence of LBBB tended to be higher in patients with HF hospitalization than in those without, whereas for RBBB it was the reverse. The temporal increase in PR interval was significantly longer and the incremental rate of the PR interval was significantly higher in patients with HF hospitalization than in those without. The temporal increase in QRS duration was significantly longer and the incremental rate of QRS duration was significantly higher in patients with HF hospitalization than in those without.

Of the total patients enrolled, 43 and 8, respectively, developed AF and second- or third-degree atrioventricular block during the follow-up, and the PR interval failed to be measured in them, so they were excluded when the long-term prognosis was evaluated. Therefore, the final study sample in this analysis consisted of 407 patients (men, 300 [73.7%]; mean age, 57.4±15.1 years). **Figure 1** shows the Kaplan-Meier estimates of the probability of freedom from HF hospitalization. The temporal incremental rate of QRS duration of 3 ms/year or greater was associated with a significantly increased risk of HF hospitalization than that of <3 ms/year (hazard ratio [HR], 2.5; 95% confidence interval [CI], 1.66–3.87; P<0.0001) (**Figure 1A**). The temporal incremental rate of PR interval of 2 ms/year or greater was associated with a significantly increased risk of HF hospitalization than that of <2 ms/year (HR, 3.4; 95% CI, 2.22–5.23; P<0.0001) (**Figure 1B**). Furthermore, when present together, the temporal incremental rate of QRS duration and PR interval potentiated each other, leading to much higher rate of hospitalization for HF (HR, 6.0; 95% CI, 3.45–10.67; P<0.0001) (**Figure 1C**). **Table 3** shows the univariate and multivariate analyses in association with HF hospitalization. The temporal incremental rate of QRS duration and PR interval was significantly associated with HF hospitalization, even after exclusion of nodal-blocking drugs. Both ECG variables were independent of age, sex, and heart rate. Confounding diseases were not associated with HF hospitalization.

Cardiovascular Mortality A total of 16 patients died of cardiovascular causes during the follow-up: 12 from HF, 2 from ventricular tachyarrhythmia, 1 from cerebral hemorrhage, and 1 from occlusion of the celiac artery. At baseline, age was not significantly different between patients with and without cardiovascular death (63.3±11.8 vs. 57.7±14.7 years; P=0.14), nor was the sex prevalence between the 2 groups (88 vs. 74% male; P=0.19). The prevalence of cardiomyopathy was significantly higher in patients with cardiovascular death than in those without (18.8 vs. 2.5%; P=0.01), but the prevalence of ischemic heart disease, valvular heart disease, AF, and diabetes was not significantly different between the 2 groups. The prevalence of various arrhythmias excluding AF was marginally higher in patients with cardiovascular death than in those without (P=0.09). The follow-up period was not significantly different between patients with and without cardiovascular death (10.9±4.9 vs. 13.4±6.4 years, P=0.13). **Table S2** shows

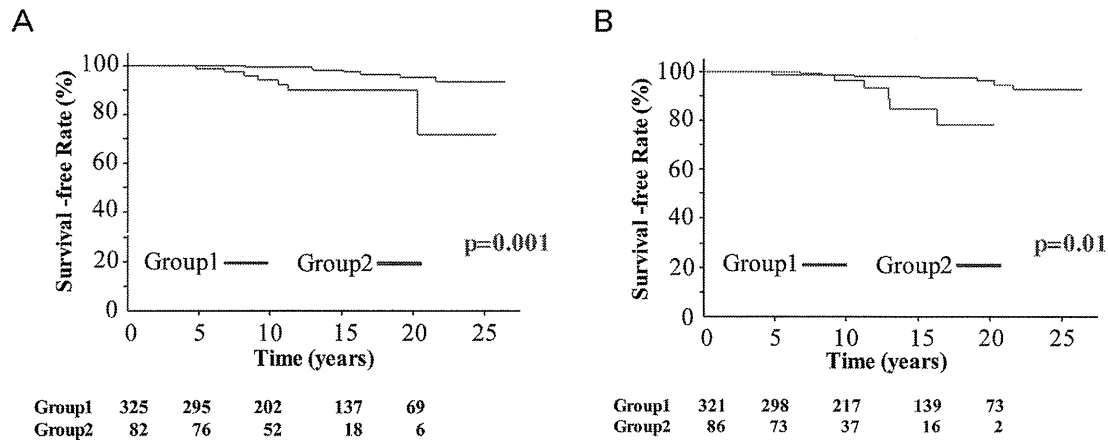

Figure 2. Kaplan-Meier survival analysis for cardiovascular mortality. (**A**) QRS-duration incremental rate <5 ms/year (Group 1) vs. ≥5 ms/year (Group 2). (**B**) PR-interval incremental rate <4 ms/year (Group 1) vs. ≥4 ms/year (Group 2). Numbers of subjects at risk are shown under each graph.

Table 4. Univariate and Multivariate Survival Analyses of Cardiovascular Mortality

	Univariate analysis (n=407)		Multivariate analysis (n=407)*		Multivariate analysis except nodal-blocking drugs (n=337)†	
	P value	HR (95% CI)	P value	HR (95% CI)	P value	HR (95% CI)
Age (<61 years=1)	0.10	2.44 (0.86–7.50)	0.30	1.82 (0.59–5.95)	0.97	1.02 (0.27–3.92)
Sex (female=1)	0.17	2.56 (0.71–16.37)	0.16	2.72 (0.71–18.00)	0.49	1.81 (0.37–14.13)
Heart rate (<66 beats/min=1)	0.98	1.01 (0.35–2.82)	0.54	0.71 (0.23–2.13)	0.67	1.34 (0.34–5.41)
Incremental rate of QRS duration (<5 ms/year=1)	0.004	5.04 (1.72–14.49)	0.06	3.18 (0.95–10.61)	0.03	4.31 (1.19–16.50)
Incremental rate of PR interval (<4 ms/year=1)	0.005	5.63 (1.76–17.62)	0.17	2.39 (0.69–8.21)	0.02	6.90 (1.47–36.96)

*Adjusted for age, sex, heart rate, LBBB, arrhythmias except AF, incremental rate of QRS duration, incremental rate of PR interval, diabetes mellitus, and cardiomyopathy.
†Adjusted for age, sex, heart rate, arrhythmias except AF, incremental rate of QRS duration, incremental rate of PR interval, and cardiomyopathy.
Abbreviations as in Tables 1–3.

the ECG characteristics. In the first ECG, heart rate, PR interval, and QRS duration did not differ between patients with and without cardiovascular death. The prevalence of LBBB was significantly higher in patients with cardiovascular death than in those without; but the prevalence of other abnormal intraventricular conductions did not differ between the 2 groups. The temporal increase in PR interval and the incremental rate of PR interval were significantly greater in patients with cardiovascular death than in those without. The temporal increase in QRS duration was not significantly different between patients with and without cardiovascular death, but the incremental rate of QRS duration was significantly higher in patients with cardiovascular death than in those without.

Long-term prognosis was analyzed after excluding patients who developed AF and second- or third-degree atrioventricular block, being evaluated in 407 patients. In **Figure 2**, the Kaplan-Meier estimates of the probability of freedom from cardiovascular mortality indicate that the temporal incremental rate of QRS duration of 5 ms/year or greater was associated with a significantly increased risk of cardiovascular mortality than that of <5 ms/year (HR, 5.0; 95% CI, 1.72–14.49; P=0.004) (**Figure 2A**). The temporal incremental rate of PR interval of 4 ms/year or greater was associated with a significantly increased risk of cardiovascular mortality than that of <4 ms/year (HR, 5.6; 95% CI, 1.76–17.62; P=0.005) (**Figure 2B**). **Table 4** shows the univariate and multivariate survival analyses in association with cardiovascular death. The temporal incremental rate of QRS duration and PR interval was significantly associated with cardiovascular mortality after exclusion of nodal-blocking drugs. Both ECG variables were independent of age, sex, and heart rate. Confounding diseases were not associated with cardiovascular mortality.

All-Cause Mortality A total of 59 patients (12.9%) died during the follow-up: 16 from cardiovascular death as noted earlier, 24 from malignant disorders, 6 from severe infection, and 13 from other causes. At baseline, age was significantly higher in patients with all-cause death than in those without (63.4±10.8 vs. 57.1±15.0 years; P=0.002), but the sex prevalence was not significantly different between the 2 groups (80% vs. 74% male; P=0.32). The prevalences of cardiomyopathy and malignant disease were significantly higher in patients with all-cause death than in those without (P<0.05 for each), but the prevalences of ischemic heart disease, valvular heart disease, diabetes, and AF were not significantly different

Table 5. Univariate and Multivariate Analyses of All-Cause Death

	Univariate analysis (n=407)		Multivariate analysis (n=407)*		Multivariate analysis except nodal-blocking drugs (n=337)†	
	P value	HR (95% CI)	P value	HR (95% CI)	P value	HR (95% CI)
Age (<61 years=1)	<0.0001	3.40 (1.89–6.35)	0.0002	3.36 (1.76–6.65)	0.01	2.64 (1.30–5.47)
Sex (female=1)	0.44	1.28 (0.69–2.56)	0.32	1.40 (0.73–2.84)	0.17	1.68 (0.81–3.84)
Heart rate (<66 beats/min=1)	0.50	1.21 (0.70–2.11)	0.39	1.29 (0.72–2.32)	0.52	1.24 (0.65–2.37)
Incremental rate of QRS duration (<5 ms/year=1)	0.004	2.59 (1.38–4.66)	0.05	1.95 (0.99–3.66)	–	–
Incremental rate of PR interval (<4 ms/year=1)	0.003	2.92 (1.48–5.49)	0.39	1.37 (0.65–2.75)	0.15	1.87 (0.79–4.19)
Malignant disease (no malignancy=1)	0.004	4.09 (1.65–8.78)	0.02	3.27 (1.25–7.47)	0.02	4.03 (1.41–9.97)

*Adjusted for age, sex, heart rate, AF, nodal-blocking drugs, incremental rate of QRS duration, incremental rate of PQ interval, cardiomyopathy, and malignant disease.
†Adjusted for age, sex, heart rate, incremental rate of PQ interval, cardiomyopathy, and malignant disease.
Abbreviations as in Tables 1,3.

between the 2 groups. The follow-up period was marginally different between patients with and without all-cause death (11.8±5.9 vs. 13.5±6.4 years, P=0.05). Table S3 shows the ECG characteristics. In the baseline ECG, heart rate, PR interval, and QRS duration was not significantly different between patients who died and those who survived. The prevalence of abnormal intraventricular conduction was not significantly different between patients who died and survived. The temporal increase in PR interval and the incremental rate of PR interval was not significantly different between patients who died and those who survived. The temporal increase in QRS duration was not significantly different between patients who died and those who survived, but the incremental rate of QRS duration was significantly higher in patients who died than in those who survived.

Long-term prognosis was analyzed after excluding the patients who developed AF and second- or third-degree atrioventricular block, being evaluated in 407 patients. Table 5 shows the univariate and multivariate survival analyses in association with all-cause death. Advanced age and malignant diseases were independently associated with all-cause mortality even after exclusion of nodal-blocking drugs. Neither the temporal incremental rate of QRS duration nor the temporal incremental rate of PR interval was independently associated with cardiovascular mortality. In addition, sex, heart rate, and confounding diseases except malignancy were not associated with all-cause mortality.

Discussion

Historically, in the 19th century Adams and Stokes separately reported a patient who suffered fainting episodes with slow pulse rate. Congenital heart block and familial occurrence of atrioventricular conduction block were subsequently noted,[8,9] suggesting inherited conduction disorders. PCCD was initially reported as an electrical conduction disorder.[10] Familial clustering of conduction system degeneration has led to the discovery of novel mutations resulting in PCCD in the absence of structural heart disease.[11] To date, multiple molecular defects responsible for PCCD have been found.[12] In addition, congenital heart diseases are accompanied by functional abnormalities of the conduction system,[13] and overlap of PCCD with structural heart diseases such as cardiomyopathy has been reported.[14,15] Neuromuscular disorders are also associated with the development of PCCD.[16] Taken together, PCCD appears not to be a single clinical entity caused by a single-gene mutation. We expand the concept of PCCD to include various cardiac diseases. In our large hospital-based population, the major findings of PCCD are summarizes as follows: (1) the temporal incremental rate of PR interval was independently associated with increased risk of HF hospitalization and cardiovascular mortality, (2) the temporal incremental rate of QRS duration was independently associated with increased risk of HF hospitalization and cardiovascular mortality, and thus (3) the severity of PCCD was intimately associated with an adverse prognosis.

Pathophysiology of PCCD

The cardiac impulse originating from the sinus node activates the atria and the ventricle, with the specialized conduction system depolarized first and the working myocardium secondarily depolarized. For impulse propagation in both the atrium and ventricle, the voltage-gated sodium channel and gap junctions are of major importance, because the former determines the excitability of the cells and the latter serves as the depolarizing current transmitted from cell to cell. Lev and Unger[1] and Lenègre[2] reported the association of excessive interstitial fibrosis near and in the specialized conduction system with PR-interval prolongation and QRS-duration widening in postmortem examinations. Their findings suggested that interstitial fibrosis played a significant role in activation delay in patients with PCCD. Familial clustering of cardiac conduction disturbance, which occur in the absence of structural heart disease or systemic disease, results from mutations in cardiac ion channel genes and associated or modifying proteins such as cytoskeletal proteins. The SCN5A mutation that results in nonfunctional human cardiac sodium channels has been found in familial PCCD.[17] This mutation consequently gives rise to slowing cardiac conduction. Besides, SCN5A has been reported as associated with dilated cardiomyopathy.[15] Therefore, structural and functional PCCDs may share the same pathophysiological background. The temporal incremental rate of QRS duration may correlate with deterioration of ventricular function, leading to increased LV filling pressures and consequently myocardial ischemia. Such longstanding conditions also may result in subendocardial fibrosis.[18] Thus, progressive widening of the QRS duration could be a surrogate for perpetual deterioration of the LV. Consistent with these pathophysiological mechanisms, the major outcome of this study was HF hospitalization.

Although most reports dealing with PCCD have consisted of small groups of patients, the presence of mutations in the

SCN5A, PRKAG2, NKX2-5 and LMNA genes, which were found to be linked to cardiomyopathies, conduction disease, and ventricular arrhythmias, has been investigated. Inter- and intraventricular conduction disturbances are the most common ECG pattern preceding the development of complete heart block, particularly in the presence of structural heart disease. Recently, it was reported that gain-of-function mutations in *TRPM4* encoding a calcium-activated nonselective cation channel of the transient receptor potential melastatin (TRPM) ion channel cause autosomal dominant isolated cardiac conduction disease.[19] In the present study, the temporal deterioration in supraventricular and ventricular conduction was independently associated with a worse prognosis of PCCD. Although gene analysis was not performed in this study, further investigation is needed to clarify whether gene mutation exists to stratify the risk of PCCD in our cohort.

Prognosis

General Population In the Framingham study,[20] the prevalence of BBB was related to aging and was more common among men than among women. Some studies report that there is no significant relation between BBB and mortality in the general population.[21–24] Regarding newly occurred BBB, left BBB was associated with an increased risk of developing overt cardiovascular disease and increased cardiac mortality.[25,26] These studies suggest that progressive degeneration of the cardiac myocardium might coincide with the development of BBB.

Medical Population In the medical population, prolonged QRS duration is reported to be a significant and independent predictor of cardiovascular mortality.[4] Several studies have shown that both left and right BBB are associated with increased mortality among patients with structural heart diseases.[27–29] In myocardial infarction, patients with BBB presented significantly more often with congestive HF and higher mortality than do their counterparts without BBB.[30] Prolonged QRS duration is also associated with decreased left ventricular systolic function and poor prognosis in patients with coronary artery disease.[6] These studies indicate that QRS duration matters a great deal for the prognosis of patients with cardiovascular diseases.

Though the follow-up period was not long, serial ECG recordings have revealed that an increase in QRS duration is associated with adverse outcomes in patients with HF.[31,32] Biventricular pacing therapy for HF that corrected the mechanical dyssynchrony caused by ventricular conduction disturbance provides evidence that patients with prolonged QRS duration have a higher susceptibility to improving their physical status by cardiac resynchronization therapy.[33] Along with these studies, the present study elucidated that the temporal incremental rate of QRS duration was independently associated with long-term poor prognosis. In addition, this study underscored the independent association between the temporal incremental rate of PR interval and QRS duration. Patients who developed AF during the follow-up were not enrolled in this study, because serial change in the PR interval was not able to be measured in those patients. Therefore, the results of this study might underestimate the prognosis of PCCD, because AF can be regarded as advanced stage of atrial conduction delay.

In this hospital-based cohort, the endpoints were determined by analysis of detailed medical records in which the prognostic outcomes were identified according to ICD codes, so our data were reliable during the long-term follow-up period. In addition, medical records are useful for evaluating physical conditions not only at 1 time point but also during follow-up, thus we precisely reviewed the medical records of all patients enrolled throughout the follow-up period.

Study Limitations

Because this cohort study was not prospectively conducted using ECG recordings, several limitations are inherent. First, we determined the increase of the PR interval and QRS duration by averaging their temporal variations. Those increases might not be temporally constant. To avoid excess change during a short time, we used ECGs for which the recording interval was more than 1 year. Second, the temporal increment rate of the PR interval was a few milliseconds. Although the temporal increment rate of the PR interval was used to stratify the prognostic outcomes, the effect of autonomic tone on the PR interval was not negligible. Third, intermittent BBB might have been missed unless the ECG finding was recorded in the hospital. Because no intermittent BBB could be documented during the follow-up in patients enrolled in this study, it is thought that intermittent BBB rarely occurred in this hospital-based population. Fourth, we did not involve cardiac functions such as left ventricular ejection fraction and mitral regurgitation. Lastly, because our study included patients who underwent ECG recording in our hospital, the risk of HF hospitalization in the study population undoubtedly was greater than that in the general population. Therefore, this factor should be considered when our results are extrapolated to a broader population.

Study Implications

PCCD was primarily identified as a cardiac electrical disease representing temporal prolongation of the QRS duration. Although prolonged QRS duration is known to be associated with adverse prognosis, the prognosis of PCCD remains unclear in a large population. This study demonstrated that patients with a higher degree of PCCD have a worse prognosis. The independent relationship between PCCD and HF hospitalization and between PCCD and cardiovascular mortality helps find patients who are at risk. The increased risk of HF hospitalization associated with the temporal incremental rate of QRS duration suggests a possible role for cardiac resynchronization therapy, particularly among patients with systolic HF. Therefore, our results indicate that careful follow-up of the ECG deserves attention for determining which patients are most likely to benefit from preventive HF therapy such as diuretics. For example, when patients visit cardiology clinics, repetitive ECG recordings might provide a noninvasive means of identifying those at high risk for worsening of HF. To make the temporal variation of the PR interval and QRS duration clinically available for treatment of patients at the early stage, improvements in the software for automatic display of these ECG variables are needed.

Acknowledgments

The authors thank Seiichi Fujisaki, Akihiko Ejima, and Tatsumi Uchiyama (GE Yokokawa Medical System Co) for their technical assistance.

Disclosures

None.

References

1. Lev M, Unger PN. The pathology of the conduction system in acquired heart disease. I: Severe atrioventricular block. *AMA Arch Pathol* 1955; **60:** 502–529.
2. Lenegre J. Etiology and pathology of bilateral bundle branch block

in relation to complete heart block. *Prog Cardiovasc Dis* 1964; **6:** 409–444.
3. Holm H, Gudbjartsson DF, Arnar DO, Thorleifsson G, Thorgeirsson G, Stefansdottir H, et al. Several common variants modulate heart rate, PR interval and QRS duration. *Nat Genet* 2010; **42:** 117–122.
4. Desai AD, Yaw TS, Yamazaki T, Kaykha A, Chun S, Froelicher VF. Prognostic significance of quantitative QRS duration. *Am J Med* 2006; **119:** 600–606.
5. Bode-Schnurbus L, Bocker D, Block M, Gradaus R, Heinecke A, Breithardt G, et al. QRS duration: A simple marker for predicting cardiac mortality in ICD patients with heart failure. *Heart* 2003; **89:** 1157–1162.
6. Murkofsky RL, Dangas G, Diamond JA, Mehta D, Schaffer A, Ambrose JA. A prolonged QRS duration on surface electrocardiogram is a specific indicator of left ventricular dysfunction [see Comment]. *J Am Coll Cardiol* 1998; **32:** 476–482.
7. Moss AJ, Zareba W, Hall WJ, Klein H, Wilber DJ, Cannom DS, et al. Prophylactic implantation of a defibrillator in patients with myocardial infarction and reduced ejection fraction. *N Engl J Med* 2002; **346:** 877–883.
8. Trevino AJ, Beller BM. Conduction disturbances of the left bundle branch system and their relationship to complete heart block. II: A review of differential diagnosis, pathology and clinical significance. *Am J Med* 1971; **51:** 374–382.
9. Schaal SF, Seidensticker J, Goodman R, Wooley CF. Familial right bundle-branch block, left axis deviation, complete heart block, and early death: A heritable disorder of cardiac conduction. *Ann Intern Med* 1973; **79:** 63–66.
10. Smits JP, Veldkamp MW, Wilde AA. Mechanisms of inherited cardiac conduction disease. *Europace* 2005; **7:** 122–137.
11. Benson DW, Wang DW, Dyment M, Knilans TK, Fish FA, Strieper MJ, et al. Congenital sick sinus syndrome caused by recessive mutations in the cardiac sodium channel gene (SCN5A). *J Clin Invest* 2003; **112:** 1019–1028.
12. Wolf CM, Berul CI. Inherited conduction system abnormalities: One group of diseases, many genes. *J Cardiovasc Electrophysiol* 2006; **17:** 446–455.
13. Schott JJ, Benson DW, Basson CT, Pease W, Silberbach GM, Moak JP, et al. Congenital heart disease caused by mutations in the transcription factor NKX2-5. *Science* 1998; **281:** 108–111.
14. Nguyen TP, Wang DW, Rhodes TH, George AL Jr. Divergent biophysical defects caused by mutant sodium channels in dilated cardiomyopathy with arrhythmia. *Circ Res* 2008; **102:** 364–371.
15. Wilde AA, Brugada R. Phenotypical manifestations of mutations in the genes encoding subunits of the cardiac sodium channel. *Circ Res* 2011; **108:** 884–897.
16. Bonne G, Di Barletta MR, Varnous S, Becane HM, Hammouda EH, Merlini L, et al. Mutations in the gene encoding lamin A/C cause autosomal dominant Emery-Dreifuss muscular dystrophy. *Nat Genet* 1999; **21:** 285–288.
17. Schott JJ, Alshinawi C, Kyndt F, Probst V, Hoorntje TM, Hulsbeek M, et al. Cardiac conduction defects associate with mutations in SCN5A. *Nat Genet* 1999; **23:** 20–21.
18. Aoki T, Fukumoto Y, Sugimura K, Oikawa M, Satoh K, Nakano M, et al. Prognostic impact of myocardial interstitial fibrosis in non-ischemic heart failure: Comparison between preserved and reduced ejection fraction heart failure. *Circ J* 2011; **75:** 2605–2613.
19. Liu H, El Zein L, Kruse M, Guinamard R, Beckmann A, Bozio A, et al. Gain-of-function mutations in TRPM4 cause autosomal dominant isolated cardiac conduction disease. *Circ Cardiovasc Genet* 2010; **3:** 374–385.
20. Kreger BE, Anderson KM, Kannel WB. Prevalence of intraventricular block in the general population: The Framingham study. *Am Heart J* 1989; **117:** 903–910.
21. Eriksson P, Hansson PO, Eriksson H, Dellborg M. Bundle-branch block in a general male population: The study of men born 1913. *Circulation* 1998; **98:** 2494–2500.
22. Fleg JL, Das DN, Lakatta EG. Right bundle branch block: Long-term prognosis in apparently healthy men. *J Am Coll Cardiol* 1983; **1:** 887–892.
23. Liao YL, Emidy LA, Dyer A, Hewitt JS, Shekelle RB, Paul O, et al. Characteristics and prognosis of incomplete right bundle branch block: An epidemiologic study. *J Am Coll Cardiol* 1986; **7:** 492–499.
24. Fahy GJ, Pinski SL, Miller DP, McCabe N, Pye C, Walsh MJ, et al. Natural history of isolated bundle branch block. *Am J Cardiol* 1996; **77:** 1185–1190.
25. Schneider JF, Thomas HE Jr, Kreger BE, McNamara PM, Kannel WB. Newly acquired left bundle-branch block: The Framingham study. *Ann Intern Med* 1979; **90:** 303–310.
26. Schneider JF, Thomas HE, Kreger BE, McNamara PM, Sorlie P, Kannel WB. Newly acquired right bundle-branch block: The Framingham study. *Ann Intern Med* 1980; **92:** 37–44.
27. Hindman MC, Wagner GS, JaRo M, Atkins JM, Scheinman MM, DeSanctis RW, et al. The clinical significance of bundle branch block complicating acute myocardial infarction. 1: Clinical characteristics, hospital mortality, and one-year follow-up. *Circulation* 1978; **58:** 679–688.
28. Ricou F, Nicod P, Gilpin E, Henning H, Ross J Jr. Influence of right bundle branch block on short- and long-term survival after acute anterior myocardial infarction. *J Am Coll Cardiol* 1991; **17:** 858–863.
29. Hesse B, Diaz LA, Snader CE, Blackstone EH, Lauer MS. Complete bundle branch block as an independent predictor of all-cause mortality: Report of 7,073 patients referred for nuclear exercise testing. *Am J Med* 2001; **110:** 253–259.
30. Melgarejo-Moreno A, Galcera-Tomas J, Garcia-Alberola A, Valdes-Chavarri M, Castillo-Soria FJ, Mira-Sanchez E, et al. Incidence, clinical characteristics, and prognostic significance of right bundle-branch block in acute myocardial infarction: A study in the thrombolytic era. *Circulation* 1997; **96:** 1139–1144.
31. Shamim W, Yousufuddin M, Cicoria M, Gibson DG, Coats AJ, Henein MY. Incremental changes in QRS duration in serial ECGs over time identify high risk elderly patients with heart failure. *Heart* 2002; **88:** 47–51.
32. Grigioni F, Carinci V, Boriani G, Bracchetti G, Potena L, Magnani G, et al. Accelerated QRS widening as an independent predictor of cardiac death or of the need for heart transplantation in patients with congestive heart failure. *J Heart Lung Transplant* 2002; **21:** 899–902.
33. Moss AJ. What we have learned from the family of multicenter automatic defibrillator implantation trials. *Circ J* 2010; **74:** 1038–1041.

Supplementary Files

Supplementary File 1

Figure S1. Temporal alterations of 12-lead ECGs in a patient with progressive cardiac conduction disease (PCCD).

Table S1. Comparison of Baseline ECG and Follow-up ECG According to Heart Failure Hospitalization

Table S2. Comparison of Baseline ECG and Follow-up ECG According to Cardiovascular Death

Table S3. Comparison of Baseline ECG and Follow-up ECG According to All-Cause Death

Please find supplementary file(s);
http://dx.doi.org/10.1253/circj.CJ-12-0849

Phenotype Variability in Patients Carrying *KCNJ2* Mutations

Hiromi Kimura, MD; Jun Zhou, PhD; Mihoko Kawamura, MD; Hideki Itoh, MD, PhD; Yuka Mizusawa, MD; Wei-Guang Ding, MD, PhD; Jie Wu, PhD; Seiko Ohno, MD, PhD; Takeru Makiyama, MD, PhD; Akashi Miyamoto, MD, PhD; Nobu Naiki, MD; Qi Wang, BS; Yu Xie, BS; Tsugutoshi Suzuki, MD, PhD; Shigeru Tateno, MD, PhD; Yoshihide Nakamura, MD, PhD; Wei-Jin Zang, PhD; Makoto Ito, MD, PhD; Hiroshi Matsuura, MD, PhD; Minoru Horie, MD, PhD

Background—Mutations of *KCNJ2*, the gene encoding the human inward rectifier potassium channel Kir2.1, cause Andersen-Tawil syndrome (ATS), a disease exhibiting ventricular arrhythmia, periodic paralysis, and dysmorphic features. However, some *KCNJ2* mutation carriers lack the ATS triad and sometimes share the phenotype of catecholaminergic polymorphic ventricular tachycardia (CPVT). We investigated clinical and biophysical characteristics of *KCNJ2* mutation carriers with "atypical ATS."

Methods and Results—Mutational analyses of *KCNJ2* were performed in 57 unrelated probands showing typical (≥2 ATS features) and atypical (only 1 of the ATS features or CPVT) ATS. We identified 24 mutation carriers. Mutation-positive rates were 75% (15/20) in typical ATS, 71% (5/7) in cardiac phenotype alone, 100% (2/2) in periodic paralysis, and 7% (2/28) in CPVT. We divided all carriers (n=45, including family members) into 2 groups: typical ATS (A) (n=21, 47%) and atypical phenotype (B) (n=24, 53%). Patients in (A) had a longer QUc interval [(A): 695±52 versus (B): 643±35 ms] and higher U-wave amplitude (0.24±0.07 versus 0.18±0.08 mV). C-terminal mutations were more frequent in (A) (85% versus 38%, $P<0.05$). There were no significant differences in incidences of ventricular tachyarrhythmias. Functional analyses of 4 mutations found in (B) revealed that R82Q, R82W, and G144D exerted strong dominant negative suppression (current reduction by 95%, 97%, and 96%, respectively, versus WT at −50 mV) and T305S moderate suppression (reduction by 89%).

Conclusions—*KCNJ2* gene screening in atypical ATS phenotypes is of clinical importance because more than half of mutation carriers express atypical phenotypes, despite their arrhythmia severity. **(*Circ Cardiovasc Genet*. 2012; 5:344-353.)**

Key Words: CPVT ■ ion channels ■ Andersen-Tawil syndrome ■ KCNJ2 ■ phenotype

Andersen-Tawil syndrome (ATS) represents a disease entity characterized by 3 features: (1) ventricular arrhythmias with Q(T)U prolongation, (2) periodic paralysis, and (3) dysmorphic features.[1,2] It is an autosomal-dominant inherited disease resulting from a heterozygous mutation of the *KCNJ2* gene. This gene encodes an inward rectifier K channel (Kir2.1), ubiquitously expressed in the myocardium, skeletal muscle, brain, and osteocytes.[3] Since the first discovery of a mutation in this disease in 2001,[4] we have extensively examined *KCNJ2* mutations in patients suspected of having ATS.[5–7] In 2007, we described both the clinical and genetic features of 23 patients (13 probands and 10 family members) and reported that the identification rate of *KCNJ2* mutation in this cohort was 100% if the patients satisfied ≥2 features of ATS.[8] On a closer inspection, however, we noticed that ≈30% of the *KCNJ2* mutation carriers lacked 2 of the ATS features: frequent PVC, bidirectional or polymorphic ventricular tachycardias (bVT or pVT), with QT or QU prolongation, without periodic paralysis or dysmorphic features. Recently, Tester et al[9] reported a possible phenotypic overlap between ATS and catecholaminergic polymorphic VT (CPVT). CPVT is a form of inherited cardiac arrhythmia,

Received November 23, 2011; accepted April 18, 2012.

From the Department of Cardiovascular and Respiratory Medicine (H.K., J.Z., M.K., H.I., Y.M., J.W., S.O., A.M., N.N., Q.W., M.I., M.H.) and the Department of Physiology (W.-G.D., Y.X., H.M.), Shiga University of Medical Science, Otsu, Japan; the Department of Cardiovascular Medicine, Kyoto University Graduate School of Medicine, Kyoto, Japan (T.M.); the Department of Pediatric Electrophysiology, Osaka City General Hospital, Osaka, Japan (T.S.); the Department of Pediatrics, Chiba Cardiovascular Center, Ichihara, Japan (S.T.); the Department of Pediatrics, Kinki University Faculty of Medicine, Higashiosaka, Japan (Y.N.); and the Department of Pharmacology, Xi'an Jiaotong University, College of Medicine, Xi'an, China (J.Z., W.-J.Z.).

Correspondence to Minoru Horie, MD, PhD, Department of Cardiovascular and Respiratory Medicine, Shiga University of Medical Science, Seta-Tsukinowa, Otsu, Shiga, 520-2192 Japan. E-mail horie@belle.shiga-med.ac.jp

Circ Cardiovasc Genet **is available at http://circgenetics.ahajournals.org** **DOI: 10.1161/CIRCGENETICS.111.962316**

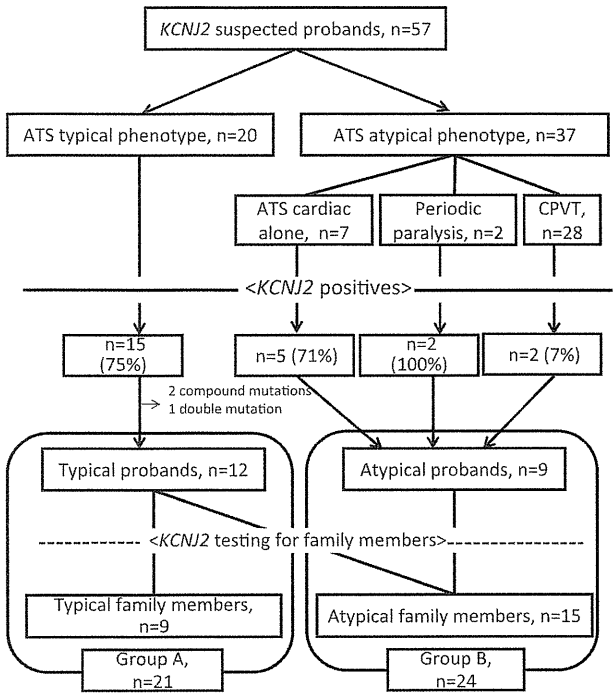

Figure 1. A Flow Chart of 57 probands suspected as carriers of *KCNJ2* mutations. ATS indicates Andersen-Tawil syndrome; CPVT, catecholaminergic polymorphic ventricular tachycardia.

characterized by exercise- and/or stress-induced p/bVTs with a normal cardiac structure.[10] However, the incidence and clinical characteristics of atypical ATS and *KCNJ2*-related CPVT remain unknown.

Clinical Perspective on p 353

In the present study, we conducted the genetic screening for *KCNJ2* mutation-related phenotypes—those fulfilling at least 1 of the ATS features or CPVT criteria. We compared the clinical and genetic features between typical ATS and atypical phenotype (only 1 of the ATS features or CPVT) patients. We hypothesized that the mutated channel function found in patients with atypical ATS phenotypes would show different I_{K1} current properties. Using the patch-clamp technique, we examined the functional features of four mutations found in the atypical phenotype group.

Methods

Study Subjects

Fifty-seven unrelated probands (65% females, age at diagnosis: 18±12 years old) from 31 institutes in Japan were enrolled in the study. They were clinically diagnosed with either typical ATS (defined as patients with ≥2 ATS features) (n=20), mild ATS [those with 1 of the ATS features—cardiac arrhythmia alone (n=7), periodic paralysis with an abnormal U wave (n=2)], or CPVT (n=28) (Figure 1 and Table 1).

Three features of ATS were clinically determined as follows: (1) Cardiac involvement was determined by the presence of ventricular arrhythmias (frequent premature ventricular contractions (PVCs), bigeminy, bVT, pVT, or monomorphic VT), with prolongation of the corrected QU interval and/or a prominent U wave.(2) The presence of periodic paralysis was based on standard criteria.[11] (3) Dysmorphic features were defined by the presence of 2 or more of the following: (a) low-set ears, (b) hypertelorism (wide-set eyes), (c) a small mandible, (d) clinodactyly (permanent lateral or medial curve of a finger or toe), and (e) syndactyly (persistent webbing between fingers or toes).[12]

Twenty-eight of the 57 patients fulfilled the diagnostic criteria of CPVT—exertional syncope plus documentation of bVT or pVT during exercise or exercise tests. Patients with QT prolongation were excluded.[10]

ECG Manifestation

We measured QU intervals if there was a prominent U wave and QT intervals in cases showing no U wave. The QT interval was defined from the onset of QRS to the end of the T wave. The U wave was defined as an early diastolic deflection after the end of the T wave. The QU interval was defined from the onset of QRS to the end of the U wave. QT and QU intervals were corrected according to the Bazzett formula.[13,14] The end of the T or U wave was the point at which a tangent drawn to the steepest portion of the terminal part of the T or U wave crossed the isoelectric line.[15] Because a prominent U wave is often fused to the next PQ segment in some cases, we defined the isoelectric line as a segment connecting 2 points preceding consecutive QRS complexes. A diagnosis of QT prolongation was made if the QTc exceeded 440 ms for males and 460 ms for females, in accordance with the standard criteria.[16] Abnormal U waves were judged based on the following criteria: (a) wave amplitude ≥0.2 mV or (b) amplitude larger than preceding T wave.[8,17]

bVT was identified as a VT characterized by a beat-to-beat alternation of the QRS axis in most of the documented runs of ventricular tachycardia (>4 consecutive beats).[10] pVT was defined as the VT with an irregularly variable axis of the QRS.

DNA Isolation and Mutation Analysis

The protocol for genetic analysis was approved by the institutional ethics committee and performed under its guidelines. All patients

Table 1. Demographic Characteristics of Different Patient Cohorts: *KCNJ2* Mutation Incidence Rates (57 Probands)

		Atypical ATS (Group B)			
	Typical ATS (Group A)	ATS Cardiac Alone	ATS Periodic Paralysis Alone	CPVT	Total
Probands, n	20	7	2	28	57
Female, n (%)	13 (65)	5 (71)	0	19 (68)	37 (65)
Age, y	17±11	21±13	19±6	18±13	18±12
QT(U)c,* ms	660±90	600±106	548±77	429±65	
KCNJ2 positives, n (%)	15 (75)	5 (71)	2 (100)	2 (7)	24 (42)

ATS indicates Andersen-Tawil syndrome; CPVT, catecholaminergic polymorphic ventricular tachycardia.

*QUc interval was used in typical ATS, ATS cardiac phenotype alone, and ATS periodic paralysis alone. QTc interval was used in CPVT.

Table 2. *KCNJ2* Mutation-Carrying Probands (n=24)

	Case No.	*KCNJ2*-DNA	Protein	Age/Sex	ECG†	QTc/QUc, ms	Dysmorphism	Paralysis	Mutated Channel Function‡	Syncope/ACA	Treatment
Typical ATS phenotype (n=15)	1	118C>T	R40X*	15/F	1, 2	451/618	+	−	−	−/−	BB
	2	200G>A	R67Q	14/F	1, 2	360/626	+	+	d.n.[8]	−/−	Ib, BB
	3	244C>T	R82W KCNH2-P1093L	11/M	2	NA/NA	+	−	d.n.[9,27]	−/−	BB
	4	430G>A	G144S KCNQ1-A341V	32/F	1, 2	NA/NA	+	+	d.n.[8,12]	+/+	IV, BB
	5	436G>A	G146S	27/F	2	487/731	NA	+	d.n.[8]	−/−	BB
	6	574A>G	T192A	16/M	1	420/700	−	+	d.n.[5]	−/−	Az
	7	653G>A	R218Q	13/F	2	423/741	−	+	d.n.[8]	−/−	BB, Az
	8	653G>A	R218Q	12/F	2	434/616	+	+	d.n.[8]	−/−	Az
	9	653G>A	R218Q	12/M	1, 4	483/716	+	−	d.n.[8]	−/−	. . .
	10	652C>T	R218W	6/F	1	365/753	−	+	d.n.[4,8]	+/−	FL
	11	652C>T	R218W	11/F	3	508/701	+	−	d.n.[4,8]	−/−	Ib, BB
	12	652C>T	R218W	6/M	2	NA/NA	+	+	d.n.[4,8]	−/−	IV
	13	652C>T	R218W	19/F	2	468/681	+	−	d.n.[4,8]	+/−	BB
	14	652C>T	R218W	12/M	1, 2, 3	400/689	+	−	d.n.[4,8]	−/−	. . .
	15	238C>T	R80C*	5/M	1, 2	468/681	+	+	R80C: −	−/−	. . .
		904G>A	V302 M						V302 M: d.n., tr[12]		
ATS cardiac phenotype alone (n=5)	16	245G>A	R82Q	46/F	2, 6	553/680	−	−	d.n. Figures 4, 5	−/−	. . .
	17	244C>T	R82W	29/F	1, 2	433/672	−	−	d.n.[9,27] Figures 4, 5	−/−	BB
	18	652C>T	R218W	6/F	1, 3	427/617	−	−	d.n.[4,8]	−/−	BB
	19	652C>T	R218W	5/M	1, 3	392/707	−	−	d.n.[4,8]	−/−	IV
	20	683ins§	R228ins*‖	24/M	1, 4	498/. . .	−	−	−	−/−	Pil
Periodic paralysis alone	21	199C>T	R67W	24/M	. . .	425/625	−	+	d.n.[8]	−/−	Az
	22	1106C>A	S369X	13/M	. . .	472/600	−	+	tr[7]	−/−	. . .
CPVT	23	431G>A	G144D	32/F	3	465/NA	−	−	Figures 4, 5	+/+	BB, FL
	24	914C>G	T305S*	36/F	1, 4, 5	443/664	−	−	Figures 4, 5	+/+	BB, ICD

NA indicates not available; age, age at diagnosis; ACA, aborted cardiac arrest; CPVT, catecholaminergic polymorphic ventricular tachycardia; ICD, implantable cardioverter-defibrillator; BB, β-blocker; Ib, mexiletine; IV, verapamil; FL, flecainide; Pil, pilsicainide; and Az, acetazolamide.

*Novel mutation.

†PVC=1, bVT=2, pVT=3, VT=4, ventricular fibrillation=5, long-QT=6.

‡d.n. indicates dominant negative; tr, trafficking defect.

§683insGAAAAGCCACTTGGTGGAAGCTCATGTTCG.

‖R228insKSHLVEAHVR.

provided informed consent before the genetic analysis was carried out. Genomic DNA was isolated from leukocyte nuclei using a DNA purification kit (Maxwell Blood DNA Purification Kit, Promega, Madison, WI). Genetic screening was first performed using denaturing high-performance liquid chromatography (dHPLC WAVE System; Transgenomic, Omaha, NE).[18] Abnormal conformers were amplified via PCR, and sequencing was performed on an ABI 3130 DNA sequencer (Perkin Elmer, Foster City, CA). The cDNA sequence numbering was based on the GenBank reference sequence NM_000891.2 for *KCNJ2*. Regarding suspected CPVT probands, we also performed screening involving target mutation analysis for 34 *RyR2* gene exons (3, 8–16, 44–49, 83–84, 88–89, 91–97, and 99–105)[19,20] and all exons of the *CASQ2* gene. In addition to these 3 genes, we examined the entire coding sequence of *KCNQ1*, *KCNH2*, *SCN5A*, and *KCNE1*-5 to exclude the unexpected presence of compound mutations related to primary electric diseases.[21,22] When a mutation was detected, we examined its presence in >200 Japanese control subjects to exclude the possibility of polymorphisms. When mutations were detected in probands, we also screened their family members.

Genotype-Phenotype Correlation

Baseline clinical characteristics collected were the age at diagnosis, symptomatic episodes, and treatment. As shown in Figure 1, we divided all *KCNJ2* mutation carriers into 2 groups—a typical ATS group (group A): carriers showing 2 or more ATS features, and an atypical ATS group (group B): those showing only 1 of the ATS features or CPVT. Compound mutation and *KCNJ2* double mutation cases were excluded from analysis.

In Vitro Mutagenesis

Regarding four *KCNJ2* mutations found in group B (R82W, R82Q, G144D, and T305S), site-directed mutagenesis was used to construct mutants, as described previously.[23] Briefly, human *KCNJ2* cDNA

was subcloned into the pCMS-EGFP plasmid (Clontech, Palo Alto, CA). We engineered *KCNJ2* mutants using a site-directed mutagenesis kit, QuickChange II XL (Stratagene, La Jolla, CA). The presence of mutations was confirmed by sequencing.

Electrophysiological Experiments and Data Analysis

To assess the functional modulation of *KCNJ2* channels, we used a heterologous expression system with CHO cells.[8,24] Briefly, the cells were transiently transfected using the Lipofectamine method (Invitrogen, Carlsbad, CA), using a 1.0 μg/35 mm dish of pCMSEGFP/*KCNJ2* (wild-type [WT] and/or mutant). For electrophysiological experiments, GFP-positive cells were selected 24 to 72 hours after transfection. Current measurement was conducted using the conventional whole-cell configuration of patch-clamp techniques at 37°C, using an EPC-8 patch-clamp amplifier (HEKA Electronik; Lambrecht, Germany). Currents were evoked by 150 ms square pulses applied in 10 mV increments to potentials ranging from −140 mV to +30 mV from a holding potential of −80 mV. Pipettes were filled with a solution containing (in mmol): K-aspartate, 60; KCl, 65; KH_2PO_4, 1; $MgCl_2$, 2; EDTA, 3; ATP (dipotassium salt), 3; and HEPES, 5 (pH adjusted to 7.2 with KOH), and had a resistance of 3.0 to 5.0 mol/LΩ. The bath solution contained (in mmol): NaCl, 140; KCl, 5.4; $MgCl_2$, 0.5; $CaCl_2$, 1.8; NaH_2PO_4, 0.33; glucose, 5.5; and HEPES, 5 (pH adjusted to 7.4 with NaOH).[25]

Immunocytochemistry

The hemagglutinin (HA) epitope (YPYDVPDYA) was introduced into the pCMS-EGFP/*KCNJ2* (WT and mutants) between Ala-115 and Ser-116 (extracellular lesion between TM1 and TM2), as previously described.[8] CHO cells were transfected with 1.0 μg of plasmid DNA in 35-mm, glass-bottom dishes. Forty-eight hours later, the cells were washed twice with phosphate-buffered saline (PBS), followed by incubation with a mouse anti-HA primary antibody (1:400) (Roche Diagnostics GmbH, Mannheim, Germany) overnight at 4°C. The cells were then washed twice with PBS and incubated with an anti-mouse antibody conjugated to Alexa 568 fluor (1:400) (Molecular Probes, Eugene, OR) as a secondary antibody for 120 minutes, at room temperature. Finally, cells were washed with and immersed in PBS, and confocal imagings were obtained with a Nikon C1si (Nikon Instruments, Tokyo, Japan).

Statistical Analysis

Clinical data are expressed as the mean±SD for continuous variables. Comparisons were performed using the χ^2 test (for counts ≥5) and Fisher exact test (for counts <5) for categorical variables and Wilcoxon test for continuous variables. All analyses of the 45 *KCNJ2* mutation-positive patients and families took into account the relatedness of patients, using a mixed model for continuous data and GEE for categorical data. The electrophysiological current data are shown as mean±SEM. A value of $P<0.05$ was considered significant.

Results

Incidence and Characteristics of *KCNJ2* Mutations in Probands

We identified 16 different *KCNJ2* mutations in 24 of 57 probands (42%) (Table 1 and Figure 1). The mean QUc intervals became longer in ATS with an increasing number of ATS features. Prevalences of *KCNJ2* mutation were 75% (15/20) in typical ATS, 71% (5/7) in mild ATS with a cardiac phenotype alone, 100% (2/2) in mild ATS with periodic paralysis alone, and 7% (2/28) in CPVT.

Table 2 summarizes the genotype/phenotype of *KCNJ2* mutation-positive probands. The mean age at diagnosis of all probands was 18±12 years old. It was significantly younger (14±12 years old) in probands with typical ATS compared with those with mild ATS (21±14 years old) or the CPVT phenotype (34±3.5 years old). In 16 *KCNJ2* mutations, 13 (81%) were missense, 2 (13%) nonsense, and 1 (6%) insertion (Table 2 and Figure 2). Six were located in the N terminus, 3 in the pore region, and 9 in the C terminus. Figure 2 depicts the phenotypes and mutation sites of probands and family members. Open circles indicate mutation carriers with 2 or more ATS features (group A), and closed symbols those with atypical ATS (group B); closed circles show the ATS cardiac phenotype alone, closed triangles show periodic paralysis alone, and closed squares show the CPVT phenotype. The letter P in each symbol indicates proband. A 5-year-old boy (case 15, Table 2) was found to have double *KCNJ2* mutations, paternal V302 M, and maternal R80C. Compound mutations were detected in 2 probands: *KCNJ2* R82W plus *KCNH2* P1093L (case 3) and *KCNJ2*-G144S plus *KCNQ1*-A341V (case 4). We excluded these 3 cases from further analyses.

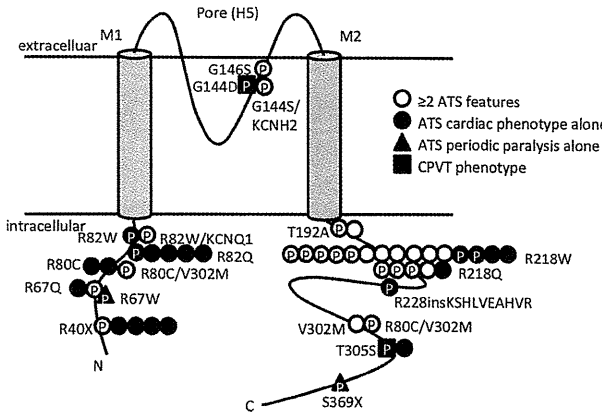

Figure 2. Topology of Kir2.1 channel showing Andersen-Tawil syndrome (ATS)-related mutation sites. **Open circles** indicate probands showing 2 or more ATS features (group A). **Closed symbols** indicate the probands in group B. **Closed circles** indicate those showing ATS with the cardiac phenotype alone; **closed triangles** are ATS with periodic paralysis alone; and **closed squares** represent a clinical diagnosis of CPVT. "P" in each symbol indicates proband.

Characteristics of *KCNJ2* Mutation Carriers

After excluding the compound mutation cases, 45 *KCNJ2* mutation carriers (27 females, 21 probands, and 24 of their mutation-positive family members) were enrolled (Table 3). Their mean age at diagnosis was 23±16 years, and the average QUc was 667±50 ms. Regarding arrhythmias, ECGs detected PVC in 30 (67%), bVT in 15 (33%), and pVT in 5 (11%) carriers. One patient had ventricular fibrillation, 4 patients (9%) had syncope, and 11 (24%) received β-blocker therapy.

Prevalence of 3 ATS Features

In 45 *KCNJ2* mutation carriers, ventricular arrhythmias (A) were found in 67% (n=30), periodic paralysis (P) in 40% (n=18), and dysmorphism (D) in 36% (n=16). Abnormal U wave (U) was positive in 88% (n=38 of 43) after excluding 2 cases whose U waves were not measured because of the presence of bigeminy. Twenty-one patients (47%) belonged

Table 3. Clinical Characteristics

	Total (n=45)	Group A (n=21)	Group B (n=24)	*P* Value
Proband, n, (%)	21	12 (57)	9 (38)	0.230
Age at diagnosis, average, y, ±SD	23±16	20±14	26±16	0.142
Female, n (%)	27 (60)	12 (57)	15 (63)	0.684
Baseline ECG				
HR, average, ms, ±SD	76±22	75±19	77±25	0.565
QTc, average, ms, ±SD	430±42	418±42	440±40	0.285
QUc, average, ms, ±SD	667±50	695±52	643±35	0.004*
T amp, average, mV, ±SD	0.51±0.27	0.56±0.28	0.46±0.26	0.215
U amp, average, mV, ±SD	0.21±0.08	0.24±0.07	0.18±0.08	0.024*
Tp-Up, average, ms, ±SD	214±31	224±32	204±28	0.151
U/T ratio, average, ±SD	0.57±0.5	0.66±0.66	0.48±0.3	0.601
Arrhythmias, patients, n (%)				
PVC	30 (67)	19 (90)	11 (46)	0.032*
Bidirectional VT	15 (33)	10 (48)	5 (11)	0.195
Polymorphic VT	5 (11)	3 (14)	2 (8)	0.368
VF	1 (2)	0	1 (4)	0.571
Cardiac events				
Syncope, patients, n (%)	4 (9)	2 (10)	2 (8)	0.891
ACA, patients, n (%)	2 (4)	0	2 (8)	0.278
Treatment				
β-blockers	11 (24)	6 (29)	5 (21)	0.589
Flecainide	2 (4)	1 (5)	1 (4)	0.924
Verapamil	2 (4)	1 (5)	1 (4)	0.925
ICD implantation	1 (2)	0	1 (4)	0.533
Mutation site				
C-terminal, patients, n (%)	27 (60)	18 (85)	9 (38)	0.002*
Pore, patients, n (%)	2 (4)	1 (5)	1 (4)	0.925
N-terminal, patients, n (%)	16 (36)	2 (10)	14 (58)	0.001*

ACA indicates aborted cardiac arrest; ICD, implantable cardioverter-defibrillator; VT, ventricular tachycardia; VF, ventricular fibrillation.

Group A: *KCNJ2* mutation carriers showing ≥2 ATS features; group B: those showing only 1 of the ATS features or catecholaminergic polymorphic ventricular tachycardia; *$P<0.05$ compared with group A.

to group A (open sections in the pie chart of Figure 3). Six of them (13%) had all 3 features, 7 (16%) both (A) and (P), 7 (16%) both (A) and (D), and 2 (5%) both (D) and (P). On the other hand, 24 patients (53%) with 1 of the ATS features belonged to group B (closed sections of Figure 3): 11 (24%) only (A), 3 (9%) only (P), 2 (4%) only (D). Eight genotype-positive family members (18%) displayed only (U).

CPVT Phenotype in *KCNJ2* Mutation Carriers

We identified 2 *KCNJ2* mutations, G144D (Table 2, case 23) and T305S (case 24), in 2 of 28 probands with CPVT phenotypes (Table 1), without dysmorphic features or periodic paralysis. These 2 cases experienced first syncope after the age of 30 (G144D, 36 years old; T305S, 32 years old). Furthermore, these probands' ECGs showed bidirectional VT at rest as well, and, as in CPVT, exercise-aggravated ventricular arrhythmia. In the G144D case, ECG always showed a PVC bigeminy even at rest, and the exercise stress test increased PVC and produced polymorphic VTs. Flecainide (150 mg per day) reduced her VTs. In the T305S case, exercise also increased numbers of PVC. She had pVT and VF while nursing her son. Her baseline ECG showed no abnormal U waves (QUc=644 ms, Tpeak-Upeak interval=185 ms).

Comparison of Patients With Typical Versus Atypical Phenotype

Table 3 summarizes the clinical characteristics of patients and compares them between groups A and B. There were no significant differences in the number of probands, age at diagnosis, and sex. Group A had a significantly longer QUc interval (group A, 695±52 ms versus group B, 643±35 ms, $P=0.004$) and higher U wave (0.24 versus 0.18 mV, $P=0.024$). PVCs were significantly more frequent in group A (n=19 patients versus n=11 patients, $P=0.032$); however, the incidences of bVT, pVT, and ventricular fibrillation were not different between the 2 groups. There were also no

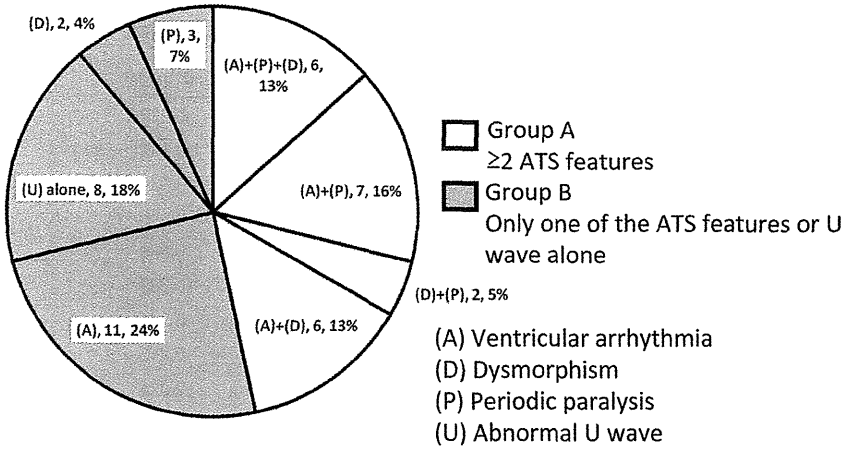

Figure 3. Prevalence of 3 features of Andersen-Tawil syndrome (ATS) among 45 *KCNJ2* mutation carriers (21 probands and 24 family members). (A) indicates ventricular arrhythmia; (P), periodic paralysis; (D), dysmorphic features; (U), abnormal U wave. **Open sections** indicate group A: patients who had ≥2 ATS features (n=21, 47%). **Closed sections** indicate group B (n=24, 53%): those who had only 1 of the ATS features or an abnormal U wave alone.

significant differences regarding the incidence of cardiac events and content of treatment.

Concerning the mutation site, C-terminal mutation carriers were more frequent in group A (n=18 versus n=9, P=0.002). In contrast, N-terminal mutations were more frequent in group B (n=2 versus n=13, P=0.001). As described above, we excluded 1 case with *KCNJ2* double mutations (Table 2, case 15) from this analysis. However his father, carrying a C-terminal mutation alone (V302 M), belonged to group A and showed a full set of ATS features. In contrast, his mother, carrying an N-terminal mutation (R80C), only displayed an abnormal U wave.

Functional Assay of 4 Mutants Found in Atypical Phenotype Group B

We conducted electrophysiological functional assays for 4 mutations in Group B—R82W, R82Q, G144D, and T305S (see Table 2; cases 16, 17, 23, and 24). Figure 4 A-a shows a family of current traces recorded from a CHO cell transfected with WT-KCNJ2 (1 μg). The lower inset in Figure 4A-a indicates the test pulse protocol. WT-*KCNJ2* expressed ample and time-independent currents showing a strong inward rectification, as depicted in the voltage-current relation in Figure 4B (closed squares). In contrast, all mutants (1 μg) were nonfunctional when expressed alone (Figure 4A-b). To simulate the allelic heterozygosity, WT and each of the mutant-*KCNJ2* clones were cotransfected at an equimolar ratio (0.5 μg each). Representative results are shown in Figure 4A-c. Outward *KCNJ2* channel currents were dominantly suppressed. In contrast, inward currents were variously reduced when coexpressed with WT.

From the results of multiple experiments, the mean current densities were measured at their respective test potentials. In Figure 4B, they are plotted as a function of the potentials, and in Figure 4C, those at −140 and −50 mV are presented as dot plots. Outward current densities at −50 mV when coexpressed with WT-KCNJ2 were 3.5±1.7 pA/pF in R82Q, 2.3±2.4 pA/pF in R82W, 2.6±0.9 pA/pF in G144D, and 8.1±2.4 pA/pF in T305S. Compared with the current densities obtained with the WT clone alone (1 μg, left plot in Figure 4C), the percent reductions were 95%, 97%, 96%, and 89%, respectively. In contrast, inward current densities at −140 mV were −162±20 pA/pF in R82Q, −152±22 pA/pF R82W, −43±13 pA/pF in G144D, and −199±20 pA/pF in T305S. Percent reductions were 58%, 39%, 89%, and 49%, respectively. Thus, G144D mutation exerted dominant negative suppression effects on both outward and inward currents. The other 3 mutations, however, had such effects only on outward currents.

Immunocytochemistry of Mutant Channels (R82Q, R82W, G144D, and T305S)

Regarding several *KCNJ2* mutations, impaired intracellular transport has been reported to cause loss of function. We therefore examined the trafficking of these 4 mutants and WT channels using an HA-tagging method. Figure 5 depicts typical results of confocal imaging. WT and HA-R82Q, HA-R82W, and HA-T305S mutants showed normal trafficking, whereas the HA-G144D mutant displayed no rim of red fluorescence, suggesting the presence of a trafficking defect.

Discussion

Prevalence of *KCNJ2* Mutation and ATS Features in Typical ATS

In the present study, we could identify heterozygous *KCNJ2* mutations in 24 (42%) of 57 probands of different cohorts showing typical ATS, and atypical phenotypes (1 of the ATS features or CPVT). Regarding 20 typical ATS (≥2 of 3 ATS features) probands, *KCNJ2* mutations were positive in 15 (75%). This value was comparable to those of previous reports: Plaster et al[4] identified 13 *KCNJ2* positives in 16 unrelated ATS kindreds (81%). Tristani-Firouzi et al[12] identified 17 *KCNJ2* positives in 25 kindreds (68%), and Donaldson et al[26] reported 9 positives in 17 kindreds (53%). The prevalence of *KCNJ2*-positive probands was, however, lower when screened in the total patients, compatible with long-QT syndrome (LQTS): Eckhardt et al[27] reported 4 *KCNJ2* mutation positives from 541 LQTS probands (0.74%). Fodstad et al reported 2 carriers in 188 LQTS patients (1%).[28]

Atypical ATS Phenotype

After excluding the compound mutation cases, there were 45 mutation carriers, and 24 (53%) had atypical ATS phenotypes and 8 had none of them. They only showed abnormal U

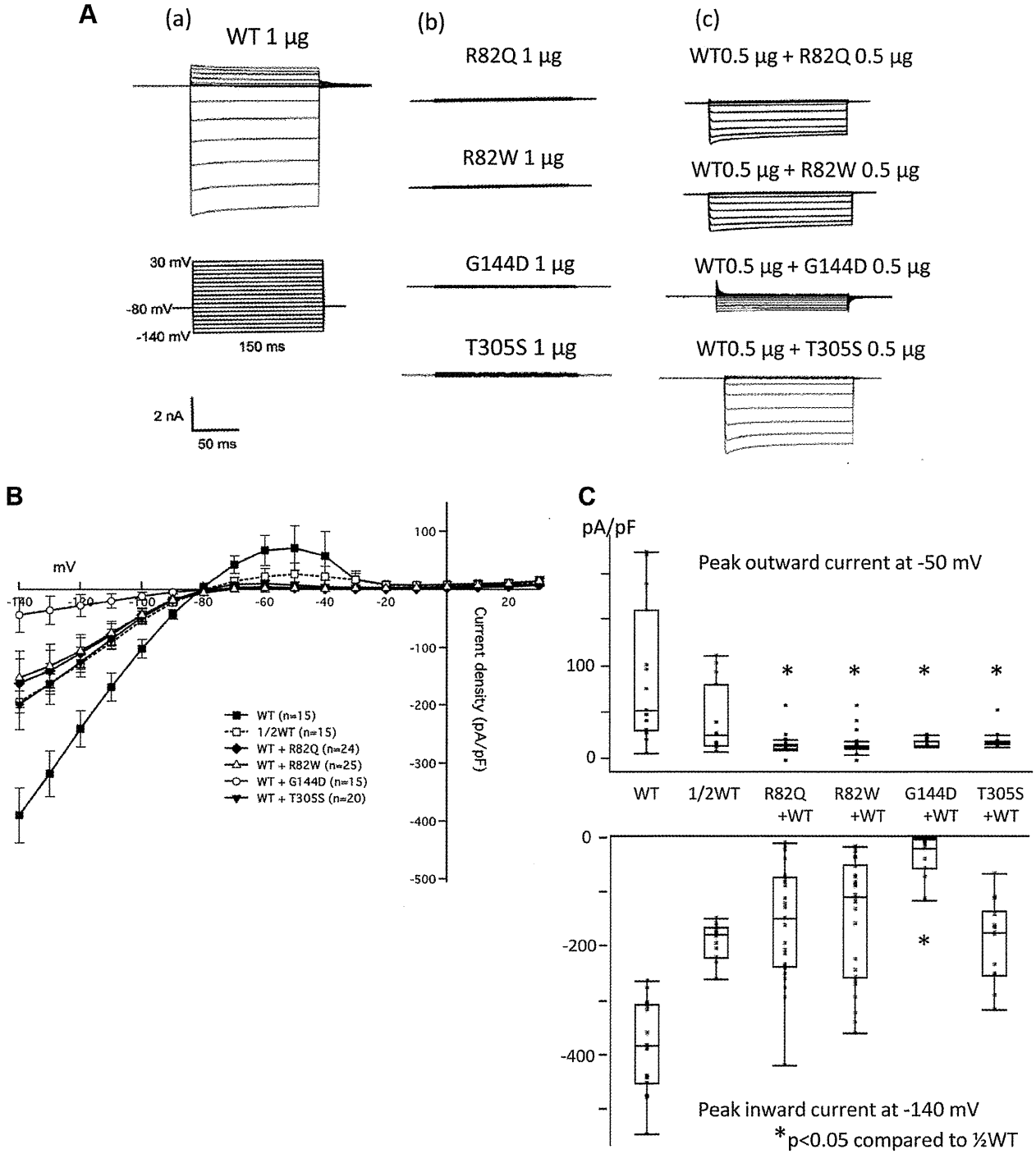

Figure 4. Functional analyses of mutated Kir2.1 channels found in group B. **A**, Representative Kir2.1 currents expressed in CHO cells: **a**, wild-type (WT) cDNA 1 μg; **b**, R82Q (1 μg), R82W (1 μg), G144D (1 μg), and T305S (1 μg). Cells were held at −80 mV. **c**, Cotransfection with WT (0.5 μg) and each mutant, R82Q (0.5 μg), R82W (0.5 μg), G144D (0.5 μg), and T305S (0.5 μg). Square pulses of 150-ms duration were applied to the potentials between −140 and +30 mV with 10-mV increments. Scale bars indicate 50 ms and 2 nA. **B**, Plots for current-voltage relationships obtained by multiple experiments of the same protocol as shown in **A**. Current densities were calculated by dividing with cell capacitance. **C**, Dot plots showing mean current densities in WT (1 μg, n=15), 1/2WT (0.5 μg, n=15), cotransfection with WT (0.5 μg) and R82Q (0.5 μg) (n=24), WT (0.5 μg) and R82W (0.5 μg) (n=25), WT (0.5 μg) and G144D (0.5 μg) (n=15), and WT (0.5 μg) and T305S (0.5 μg) (n=20). **Upper panel**, Those at −140 mV; **lower panel**, those at −50 mV.

waves. Accordingly, probands in this group received a genetic diagnosis at a significantly older age. Among the 3 features of ATS, dysmorphic features could be seen from the infant period; in contrast, ventricular arrhythmia appeared later, presumably because the I_{K1} current could be reduced in females by gonadal steroids.[29] The ATS-related phenotype was reported to be dependent on sex[30]—female subjects with *KCNJ2* R67W from a white family displayed ventricular